AGU PUBLICATIONS

Geochemistry, Geophysics, Geosystems

RESEARCH ARTICLE
10.1002/2017GC007111

Environmental Controls on Mg/Ca in *Neogloboquadrina incompta*: A Core-Top Study From the Subpolar North Atlantic

Audrey Morley[1,2], Tali L. Babila[3], James Wright[4], Ulysses Ninnemann[5], Kikki Kleiven[5], Nil Irvali[5], and Yair Rosenthal[6]

[1]School of Geography and Archaeology, National University of Ireland Galway, Galway, Ireland, [2]Ryan Institute for Environmental, Marine, and Energy Research, Galway, Ireland, [3]Earth and Planetary Sciences, University of California, Santa Cruz, Santa Cruz, CA, USA, [4]Department of Geological Sciences, Rutgers University, Piscataway, NJ, USA, [5]Department of Earth Science and Bjerknes Centre for Climate Research, University of Bergen, Bergen, Norway, [6]Department of Marine and Coastal Science and Department of Earth and Planetary Sciences, Rutgers University, New Brunswick, NJ, USA

Key Points:
- At values below 200 μmol kg^{-1}, the carbonate-ion concentration of seawater results in higher-than-expected Mg/Ca values for *N. incompta*
- The carbonate-ion concentration effect on Mg/Ca in *N. incompta* can be quantified and removed using a new correction scheme
- The effect of volcanic ash contamination on foraminiferal Mg/Ca values can be effectively removed by subtraction

Supporting Information:
- Supporting Information S1

Correspondence to:
A. Morley,
audrey.morley@nuigalway.ie

Citation:
Morley, A., Babila, T. L., Wright, J., Ninnemann, U., Kleiven, K., Irvali, N., & Rosenthal, Y. (2017). Environmental controls on Mg/Ca in *Neogloboquadrina incompta*: A core-top study from the subpolar North Atlantic. *Geochemistry, Geophysics, Geosystems*, *18*, 4276–4298. https://doi.org/10.1002/2017GC007111

Received 7 JUL 2017
Accepted 23 OCT 2017
Accepted article online 1 NOV 2017
Published online 4 DEC 2017

Abstract Magnesium/calcium paleothermometry is an established tool for reconstructing past surface and deep-sea temperatures. However, our understanding of nonthermal environmental controls on the uptake of Mg into the calcitic lattice of foraminiferal tests remains limited. Here we present a combined analysis of multiple trace element/calcium ratios and stable isotope (δ^{18}O and δ^{13}C) geochemistry on the subpolar planktonic foraminifera *Neogloboquadrina incompta* to assess the validity of Mg/Ca as a proxy for surface ocean temperature. We identify small size-specific offsets in Mg/Ca and $\delta^{18}O_c$ values for *N. incompta* that are consistent with depth habitat migration patterns throughout the life cycle of this species. Additionally, an assessment of nonthermal controls on Mg/Ca values reveals that (1) the presence of volcanic ash, (2) the addition of high-Mg abiotic overgrowths, and (3) ambient seawater carbonate chemistry can have a significant impact on the Mg/Ca-to-temperature relationship. For carbonate-ion concentrations of values $>$ 200 μmol kg^{-1}, we find that temperature exerts the dominant control on Mg/Ca values, while at values $<$ 200 μmol kg^{-1} the carbonate-ion concentration of seawater increases the uptake of Mg, thereby resulting in higher-than-expected Mg/Ca values at low temperatures. We propose two independent correction schemes to remove the effects of volcanic ash and carbonate-ion concentration on Mg/Ca values in *N. incompta* within the calibration data set. Applying the corrections improves the fidelity of past ocean temperature reconstructions.

1. Introduction

Magnesium-to-calcium (Mg/Ca) thermometry is a paleoceanographic proxy used on various geological time scales (Barker et al., 2005; Lea et al., 2002; Lear et al., 2000). For the planktonic foraminifera *Neogloboquadrina incompta*, the sensitivity of Mg/Ca to temperature was previously determined by laboratory culturing experiments (von Langen et al., 2005), core-top sediments (Elderfield & Ganssen, 2000), and sediment trap time series (Pak et al., 2004). However, current Mg/Ca calibration equations do not include oceanic temperatures below 10°C, thereby introducing uncertainties to reconstructions of colder-than-present environments. The limited data at low ocean temperatures originate from the fact that core-top Mg/Ca-temperature calibrations from the North Atlantic seldom incorporate sample sites north of 60°N (Elderfield & Ganssen, 2000). Sites north of 60°N may have been avoided for two reasons: (1) magnesium contamination from volcanic rich sediments near Iceland can compromise the accuracy and precision of Mg/Ca-paleothermometry and (2) several earlier investigations involving sites within the cold temperature habitats of both *N. incompta* and *Neogloboquadrina pachyderma* (sinistral) identified a departure of the Mg/Ca-temperature relationship in the low temperature range (Hendry et al., 2009; Kozdon et al., 2009; Meland et al., 2006). Furthermore, it has been hypothesized that in addition to temperature, carbonate-ion concentrations may exert a strong secondary effect on Mg/Ca, mainly at low concentrations associated with cold sea surface temperatures (Evans et al., 2016; Kisakürek et al., 2008; Lea et al., 1999; Russell et al., 2004).

Here we present combined Mg/Ca and stable oxygen isotope (δ^{18}O) measurements for *N. incompta* from a new data set collected from the subpolar North Atlantic, Icelandic Shelf, and Norwegian Basin, with the aim of extending the existing Mg/Ca-temperature calibration to explicitly include core-top samples in the low

temperature range (<10°C; Figure 1). The calcification conditions of most planktonic foraminifera are not representative of a discrete depth but rather represent the depth range over which calcite is precipitated during their ontogeny. For this reason, we use a paired geochemical approach to calibrate Mg/Ca of *N. incompta* to calcification temperatures based on $\delta^{18}O$ measurements from the same samples. While limitations using this approach arise at high northern latitudes, where the $\delta^{18}O$ values of seawater ($\delta^{18}O_{sw}$) are highly variable in the surface ocean, we can reduce the uncertainty by assuming a discrete calcification depth (e.g., hydrographic temperature) as both geochemical proxies imprint the same ocean temperature into their foraminiferal test geochemistry. The strength of a core-top calibration study is that samples are

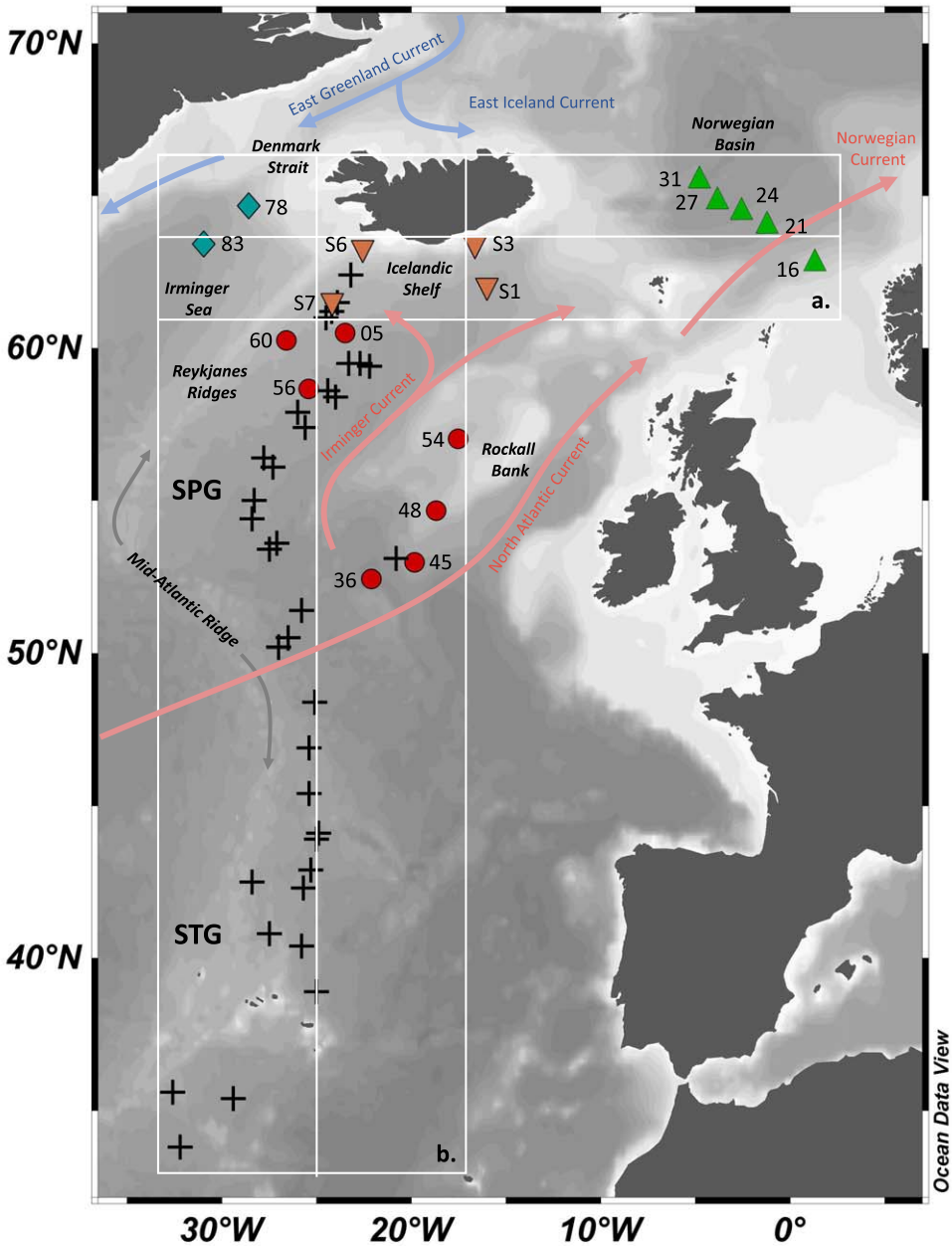

Figure 1. (Map) Map showing the locations of core sites used in this study as well as previously published core-top records for *N. incompta* by (Elderfield & Ganssen, 2000; EG) and (Yu et al., 2007; YU). Norwegian Basin (KN177-1; green upward triangles), Denmark Strait (blue diamonds), subpolar North Atlantic (KN158-4; red circles), Iceland Sea (downward orange triangles; 64PE341, LCD), and EG and YU (black crosses). Also shown are the two transect lines, (a) centered at 63.5°N going from west to east and (b) centered at 25°W going from south to north, shown in Figure 5. Map produced with Ocean Data View (Schlitzer, 2002).

representative of the dynamic conditions present in the open ocean settings and have undergone similar depositional processes to those occurring in paleoceanographic down-core records. In contrast, culture-based calibration studies (von Langen et al., 2005) afford the opportunity to isolate the influence of a single environmental variable (e.g., temperature), which is more challenging with core-top-based calibrations.

2. Materials and Methods

2.1. *Neogloboquadrina incompta* Ecology

Darling et al. (2006) show that the right-coiling form of *N. pachyderma* (dextral) is a genetically distinct species, with a different ecology and biogeographic distribution from its sinistral-coiling counterpart. We therefore follow their nomenclature suggestion and adopt the species name *N. incompta* to refer to the dextral coiling species for the remainder of this manuscript. *N. incompta* is a nonspinose species that consists of a macroperforate test texture with a notable outer crust (Srinivasan & Kennett, 1974). In some species, the formation of an outer crust is related to gametogenesis, while in others it is thought that outer crust formation is linked to colder temperatures deeper in the water column (Kohfeld et al., 1996; Srinivasan & Kennett, 1974). For *N. incompta*, it remains unclear which of the two processes is responsible for the formation of the outer crust. Currently, *N. incompta* is present in temperate, subpolar, and transitional water masses of the North Atlantic including the Norwegian Sea, Denmark Strait, and North Atlantic Current, while a second genotype variety occurs in the North Pacific (eastern North Pacific and Santa Barbara Channel; Darling et al., 2006). In the North Atlantic, the optimum temperature range for *N. incompta* is 8.5–21.4°C and is further extended to 5.8–23.6°C in areas with high carbon export production rates (Žarić et al., 2005). According to a sediment trap study from 49°11.20′N, 12°49.18′W, *N. incompta* blooms twice a year at midlatitudes, first in early summer (May/June) and again (the main bloom) between July and September. At higher latitudes, the two peaks merge into one late summer bloom (July–September) where summer sea surface temperatures (SST) are colder than 13–16°C (Chapman, 2010).

Previously, it was suggested that the preferred depth habitat for *Neogloboquadrinids* is bound to discrete isopycnal surfaces (Kozdon et al., 2009; Simstich et al., 2003). For *N. pachyderma* (*s.*), for example, Kozdon et al. (2009) identified a narrow isopycnal surface of $\sigma_t = 27.7–27.8$ as the preferred habitat for this species, suggesting that the density-driven water mass stratification is a strong factor in controlling depth habitat. Similarly, Simstich et al. (2003) demonstrated that the $\delta^{18}O_c$ values for *N. pachyderma* (*s.*) off Norway reflect water depths near and below the pycnocline in the northeastern North Atlantic. When compared to *N. pachyderma* (*s.*), *N. incompta* has been shown to be more abundant above the pycnocline, preferring shallower and warmer surface waters (Simstich et al., 2003). *N. incompta* also exhibits a strong preference for maximum chlorophyll *a* concentrations in the water column (Kuroyanagi & Kawahata, 2004). The latter observations are in line with an earlier study linking foraminiferal depth habitat preferences to maximum chlorophyll *a* concentrations in the North Atlantic water column (Fairbanks & Wiebe, 1980). Maximum chlorophyll concentrations are generally confined to the top 50 m of the water column north of 40°N latitude in the North Atlantic Ocean (O'Brien et al., 2002; Pattiaratchi et al., 1989), which agrees well with observations of *N. incompta* favoring warm stratified surface waters (Sautter & Thunell, 1989) and high-nutrient environments (Ortiz et al., 1995; Sautter & Sancetta, 1992). Later in the growing season (September–October), depth habitats of *N. incompta* may occasionally extend to 100 m depth due to the onset of wind-induced turbulent mixing of stratified surface waters and the entrainment of nitrate and chlorophyll into the mixed layer (Schiebel et al., 2001).

2.2. Sample Locations

Norwegian Basin. We selected five core-top sample sites collected using a multicorer during the KN177-1 (*RV Knorr*) cruise in 2004. The samples span depths from 967 to 3873 m and provide a depth transect down the Norwegian continental slope and into the Norwegian Basin (Table 1 and Figure 1). Surface waters at these sites are controlled by the Norwegian Current. At core sites deeper than 1,300 m planktonic foraminifera are abundant in the sediment (>30% calcium carbonate $CaCO_3$ content), while at sites shallower than 1,300 m the terrigenous component is greater and the $CaCO_3$ content may be as low as 15%. Significant downslope reworking is not observed below 500 m (Mackensen et al., 1985) and modern regional sedimentation rates are generally low (2–6 cm per thousand years; Simstich et al., 2003 and references therein).

Icelandic Shelf and Denmark Strait. Six core-top sample sites were collected from the Icelandic Shelf and Denmark Strait using a multicorer. Four sites are located east of the Reykjanes Ridges and were collected during the *RV Pelagia* cruise 64PE341 in 2011, while two core tops west of the ridge on the southern flank of the Denmark

Table 1
Geographic Locations, Ocean Depths at Core Location, and Sediment Depths Sampled

Cruise	Core	Lat (°N)	Long (°W)	Depth (m)	Sample depth (cm)	150–255 (μm) No. of replica: Mg/Ca	255–355 (μm) No. of replica: Mg/Ca	150–255 (μm) No. of replica: $\delta^{18}O_c$	250–355 (μm) No. of replica: $\delta^{18}O_c$
					Subpolar North Atlantic				
KN158-4 (*July 1998*)	MC05	60.5	23.5	1,800	0–0.5	2	0	1	1
	MC36	52.4	22.1	4,056	0.5–1.0	3	3	1	1
	MC56	58.7	25.4	2,765	0.5–1.0	3	3	1	1
	MC45	53.0	19.8	2,739	0.5–1.0	3	3	1	1
	MC54	57.0	17.5	1,330	1.0–2.0	3	3	1	1
	MC48	54.7	18.7	1,095	0.5–1.0	3	3	1	1
	MC60	60.3	26.6	1,866	0.5–1.0	2	0	1	1
					Denmark Strait				
	MC78	64.7	28.6	1,236	0.5–1.0	3	3	1	1
	MC83	63.4	31.0	2,486	0.5–1.0	3	3	1	1
					Icelandic Shelf				
64PE341 (2011)	LCD-S1	62.5	16.5	2,250	0–0.5	4	1	1	1
	LCD-S3	63.5	15.5	186	0–0.5	8	9	2	2
	LCD-S6	63.5	22.5	316	0–0.5	1	1	1	1
	LCD-S7	61.5	24.5	1,628	0–0.5	3	4	2	2
					Norwegian Basin				
KN177-1 (2004)	MC16B	62.5	−1.5	967	0–1.0	1	1	1	1
	MC21B	63.5	1.5	2,640	0–1.0	1	1	1	1
	MC24C	64.5	2.5	3,036	0–1.0	1	1	1	1
	MC27B	64.5	3.5	3,341	0–1.0	1	1	1	1
	MC31B	64.5	4.5	3,873	0–1.0	3	2	1	2

Note: Also shown are numbers of replicates analyzed for Mg/Ca and $\delta^{18}O_c$, respectively, for each size fraction, 150–255 and 255–355 μm.

Strait were collected during *RV Knorr* cruise KN158-4 in 1998. All Icelandic Shelf sites are influenced by the Irminger Current, which transports North Atlantic water (temperature $>$ 5°C, salinities $>$ 34.5‰) to the northwest. Samples located in the Denmark Strait may further be influenced by the East Greenland Current, which transports colder Arctic waters (temperature 0–2°C, salinity 34.9–35‰) southward (Hopkins, 1991; Krauss, 1995).

Subpolar and Subtropical North Atlantic. An additional six core-top sites were collected during the 1998 *RV Knorr* cruise KN158-4 from sites within the subpolar North Atlantic, and together form a north-south transect from 60°N to 52.5°N. We also augmented our data set with 35 previously published samples collected from 62.40°N to as far south as 37.10°N along the Mid-Atlantic Ridge (Elderfield & Ganssen, 2000; Yu et al., 2008). In terms of surface water characteristics, the majority of our core locations are influenced by subtropical and subpolar surface waters supplied by the North Atlantic Current, Irminger Current, and Norwegian Current (Krauss, 1986, 1995). Notable exceptions are our sites in the Denmark Strait (MC78 and MC83), which are in close proximity to Arctic water masses passing through the East Greenland Current, and the westernmost site in the Norwegian Basin (MC31), which may be influenced by recirculating Arctic water masses supplied by the East Icelandic Current (Figure 1 and Table 1).

2.3. Sample Preparation

Between 40 and 200 *N. incompta* individuals were picked from the 255–355 μm test size fraction, along with 55–400 picked from the 150–255 μm fraction. Test weights were measured using a Mettler Toledo microbalance with ±5 μg accuracy. To determine individual test weights, the total number of individuals (at least 40) measured was divided by the final weight per sample. Foraminifera tests were gently crushed between two glass plates to facilitate chemical cleaning. Subsequently, fragments were gently mixed with a 000 brush to homogenize the sample, after which three aliquots with approximately 400 μg of $CaCO_3$ were transferred to acid-leached centrifuge vials. To constrain the variability within a sample set, we included a high specimen count and took replicates whenever possible. A detailed account of measured replicates is given in Table 1.

2.4. Analytical Methods: Paired Mg/Ca-δ^{18}O Measurements

Foraminiferal tests were chemically treated following the protocol of Boyle and Keigwin (1985) to remove clays, organic matter, and metal oxides. The cleaning procedure was further modified by removing metal oxides *before* organic matter, according to Rosenthal et al. (1997). After clay removal (rinsing with Milli-Q water and glass distilled methanol), one 50–100 μg aliquot for each size fraction was used for stable oxygen and carbon isotope analysis, generally resulting in at least one isotopic measurement for three replicate Mg/Ca measurements (see Table 1 for details on replicate analysis for both Mg/Ca and isotopes). The remaining sample went through the above mentioned cleaning protocols for trace metal analysis. A final dilute-acid (0.001 N HNO_3) leach was completed, before samples were dissolved in 100 µL of 0.065 N (OPTIMA®) HNO_3 and diluted with 300 μL 0.5 N (OPTIMA®) HNO_3 to obtain a target Ca concentration of 4 ± 1 mmol L^{-1}.

Trace elements (Mg, Al, Fe, Sr, U, Mn, B, and Ca) were analyzed at the Department of Marine and Coastal Sciences at Rutgers University using a Thermo Finnigan Element XR Sector Field Inductively Coupled Plasma Mass Spectrometer (SF-ICP-MS), operated in low resolution ($m/\Delta m = 300$) and medium resolution ($m/\Delta m = 4{,}300$) following the methods outlined in Rosenthal et al. (1999) and modified later for Boron analysis by Babila et al. (2014). Element-to-calcium (El/Ca) ratios were corrected for the effects of variable sample [Ca] concentrations by analyzing a suite of six solutions, prepared by diluting an in-house-spiked gravimetric standard (SGS) with 0.5 m*M* HNO_3, to obtain Ca concentrations spanning 1.5–8 mmol L^{-1}. This range covers the expected distribution of [Ca] concentrations in our samples. Ultimately, these solutions allow us to quantify and correct for the effects of variable sample [Ca] concentrations on the accuracy of Mg/Ca measurements (so-called matrix effect; Rosenthal et al., 1999). Matrix corrections are typically < 0.1 mmol mol^{-1} Mg/Ca, which represents approximately 5–10% of Mg/Ca values. Analytical precision was determined by repeated analysis of three consistency standards over the course of this study. The long-term precision of Mg/Ca at 1.10, 2.40, and 6.10 mmol mol^{-1} concentrations were ±1.5% (RSD), ±1.5%, and ±1.2%, respectively.

Stable isotope analysis was carried out at the Department of Earth and Planetary Sciences, Rutgers University. Using a common bath introduction system attached to a Micromass Optima mass spectrometer, samples were reacted for 15 min in 90°C phosphoric acid. Stable isotope values of calcite are reported in VPDB. The 1σ precision of the NBS 19 standard analyzed during automated runs is ±0.05‰ for δ^{13}C and ±0.07‰ for δ^{18}O.

3. Description of Previously Published Geochemical Data

Previously published geochemical data incorporated into our data set were originally reported by Elderfield and Ganssen (2000) and later supplemented by Yu et al. (2008), who from hereon will be referred to as EG and YU, respectively. EG made paired measurements of test stable oxygen isotopes ($\delta^{18}O_c$) and Mg/Ca values for 21 core-top samples along a 37.10°N–62.40°N (transect samples south of 37°N were not included in this study), using approximately 20 *N. incompta* individuals of 250–355 μm size per sample. Using 60–120 individuals of the same species (size fraction 250–300 μm), YU repeated Mg/Ca measurements for 19 of these core tops and provided an additional 14 samples that can be paired to the $\delta^{18}O_c$ values reported by EG. Together, the EG and YU studies constitute a total of 35 core-top samples from the North Atlantic, and since 19 of the 33 core tops were used in both studies, duplicate Mg/Ca measurements are available for those sites.

A comparison of both the EG and YU data sets reveals that three pairs (out of 19) have significantly offset Mg/Ca ratios, with differences of 0.44, 0.47, and 0.38 mmol mol^{-1} respectively. Consequently, we excluded these pairs from further calculations. To account for the different foraminifera cleaning protocols employed by EG (Mg-cleaning; Barker et al., 2003) and YU (Cd-cleaning; Boyle & Keigwin, 1985; Rosenthal et al., 1997), we reduced Mg/Ca values from the EG data set by 21.5% to obtain the best fit ($r^2 = 0.65$, $n = 51$, $p = 0.01$) between the EG and YU Mg/Ca values, with respect to apparent calcification temperatures (see section 4.1 and supporting information Figure S2). The resultant compiled linear regression between EG and YU Mg/Ca values has an intercept of 0.02 (±0.29) and slope of 0.098 (±0.12). Previous reports of offsets due to different cleaning protocols generally range between 10% and 15% when comparing oxidative and combined oxidative and reductive treatments (Barker et al., 2003; Johnstone et al., 2016; Rosenthal et al., 2004). Furthermore, reduction of Mg/Ca values may occur due to repeated weak acid leach treatments (Barker et al., 2003), which could account for the observed 21.5% offset.

In the original publications of EG and YU, apparent calcification temperatures (ACD) were derived by comparing the measured foraminiferal $\delta^{18}O_c$ to the predicted $\delta^{18}O_c$, assuming equilibrium with seawater $\delta^{18}O$ ($\delta^{18}O_{sw}$). Surface ocean $\delta^{18}O_{sw}$ values used by EG and YU were measured during the Actuomicropaleontology Paleoceanography North Atlantic Project II (APNAP) expedition on R/V Tyro (10 April to 1 May 1988). However, a consistent offset identified by LeGrande and Schmidt (2006) between $\delta^{18}O_{sw}$ values collected during the 1998 APNAP II expedition and other cruise data led to the exclusion of the former from the Global gridded data set of the oxygen isotopic composition in seawater (LeGrande & Schmidt, 2006). Therefore, we used the LeGrande and Schmidt data set to recalculate ACDs for YU and EG.

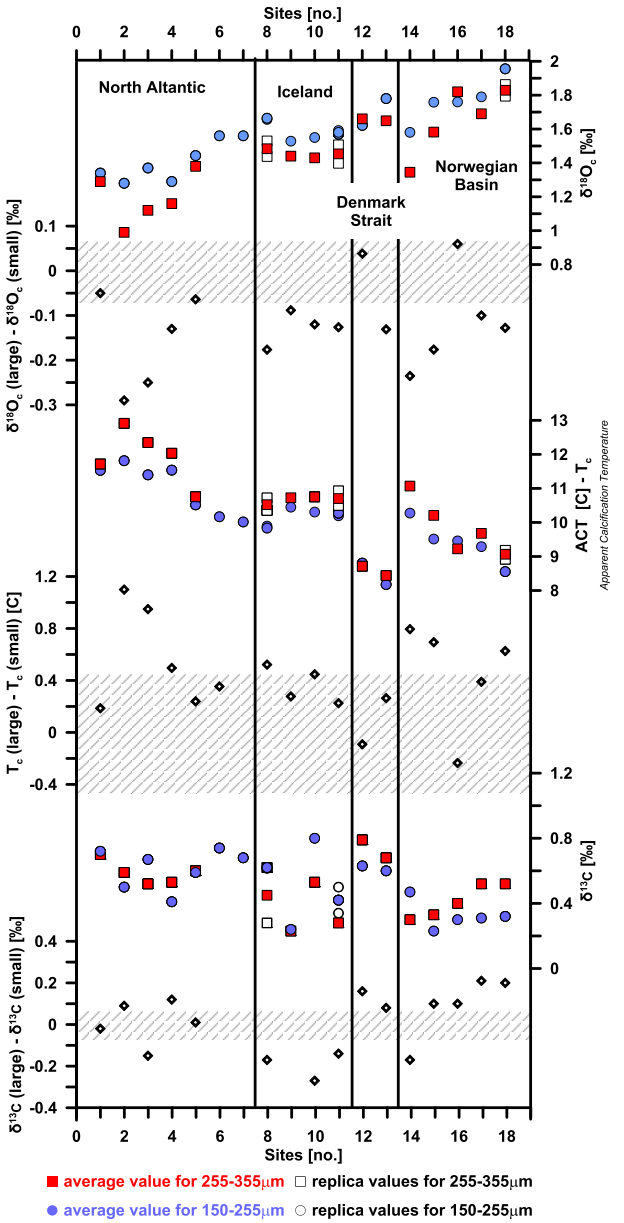

Figure 2. Plot depicting the difference in $\delta^{18}O_c$ ACT, and $\delta^{13}C$ values between different size classes. Blue circles represent average values for size fractions 150–255 μm (s, small) and red squares represent average values for size fraction 255–355 μm (l, large). White circles (150–255 μm) and white squares (255–355 μm) show replica measurements for each site. The shaded areas illustrate the uncertainty associated with respective measurements ($\delta^{18}O_c = \pm 0.07‰$; ACT = 0.45°C; $\delta^{13}C = \pm 0.05‰$). The 18 sites are grouped according to region and then by increasing latitude.

4. Results

4.1. Estimation of Apparent Calcification Depth (ACD) and Temperature (ACT)

While measured $\delta^{18}O_c$ values range from 0.99‰ to 1.96‰, we note that values are consistently lower for larger (255–355 μm) test sizes than for smaller (150–255 μm) specimens, the average difference being 0.14 (±0.072‰; Figure 2). We estimated ACT for all *N. incompta* samples (this study, EG, and YU) by comparing the measured foraminiferal $\delta^{18}O_c$ values to the expected equilibrium values of calcite ($\delta^{18}O_c$) precipitated from seawater. Water-column data needed to calculate $\delta^{18}O_c$ include temperature, salinity, and $\delta^{18}O_{sw}$. We selected temperature and salinity water-column data from the seasonal June–July–August (JJA) WOA09 0.5° gridded data set (Antonov et al., 2010; Locarnini et al., 2010). Specifically, we employed data from both the station closest to the core site and from within a 0.5° (longitude and latitude) radius to more accurately gauge locally averaged temperature and salinity values. The seasonal hydrographic data set was preferred over the annually averaged data set as it is more representative of the environmental conditions during the growing season of *N. incompta* at mid-to-high latitudes. Each site used in this study (including YU and EG) exhibit summer SST values < 15°C, indicating that the geochemical signatures (i.e., Mg/Ca, $\delta^{18}O$) recorded in core-top samples should fall in the single late-summer bloom (July–September) as suggested by Chapman (2010).

To obtain $\delta^{18}O_{sw}$ depth profiles, we used modeled water-column data from LeGrande and Schmidt (2006). As with WOA09, we retrieved data from both the closest station to each core site and within a 0.5° radius to provide locally averaged $\delta^{18}O_{sw}$ values. We then calculated site-specific $\delta^{18}O_{sw}$-salinity (annual) linear relationships for each core. For our study, this approach is preferable to using a single North Atlantic Ocean relationship owing to the often-sharp hydrographic changes that occur close to mid-to-high-latitude frontal systems. Since only annual $\delta^{18}O_{sw}$ data are available, we used the $\delta^{18}O_{sw}$-salinity (annual) linear relationships, along with seasonal WOA09 salinity values, to estimate seasonal (JJA) $\delta^{18}O_{sw}$ values for each site. This approach accounts for the importance of using seasonally averaged data rather than point measured (CTD) or annually derived data to estimate $\delta^{18}O_c$ values for core-top samples.

In order to assess which paleotemperature equation is most suitable for calculating estimated $\delta^{18}O_c$ values, we evaluated four commonly used equations, including that developed by Kim and O'Neil (1997) for inorganic calcite:

$$T = 16.1 - 4.64\left[\delta^{18}O_c - \delta^{18}O_{sw}\right] + 0.09\left[\delta^{18}O_c - \delta^{18}O_{sw}\right]^2 \quad (1)$$

the equation developed by von Langen (2001) for *N. incompta* via culturing experiments at 9–20°C temperature:

$$T = 17.2(\pm 0.4) - 6.16(\pm 0.6)\left[\delta^{18}O_c - \delta^{18}O_{sw}\right] \quad (2)$$

the benthic foraminifera equation developed by Shackleton (1974; modified after O'Neil et al., 1969):

$$T = 16.90 - 4.38\left[\delta^{18}O_c - \delta^{18}O_{sw}\right] + 0.1\left[\delta^{18}O_c - \delta^{18}O_{sw}\right]^2 \quad (3)$$

and the equation developed by Bemis et al. (2002) for low-light conditions in *Globigerina bulloides*:

$$T = 13.4 - 4.48\left[\delta^{18}O_c - \delta^{18}O_{sw}\right] \quad (4)$$

Using these $\delta^{18}O$ paleotemperature equations, we determined expected $\delta^{18}O_c$ depth profiles (0–400 m) based on seasonal (July–September) temperature, salinity, and $\delta^{18}O_{sw}$ data. Calculations were completed by subtracting 0.27‰ in order to compare measured $\delta^{18}O$ values of CO_2 produced through the reaction of calcite with H_3PO_4 to those of CO_2 equilibrated with water (Friedman & O'Neil, 1977). The depth at which the expected equilibrium $\delta^{18}O_c$ values matched the measured foraminiferal $\delta^{18}O_c$ values (determined by linear interpolation) is the apparent calcification depth (ACD), and the apparent calcification temperature (ACT) was determined based on temperatures recorded at the ACD. The error associated with ACT depends on uncertainties in the seasonal $\delta^{18}O_{sw}$ values (derived from hydrographic data using the LeGrande and Schmidt (2006) WOA09 model set) and the instrumental precision of $\delta^{18}O_c$ measurements. As discussed above, *N. incompta* calcifies at or above the pycnocline. At all sites included in our study, the base of the pycnocline is found above 150 m. The maximal $\delta^{18}O_{sw}$ change over the upper 150 m water column is 0.1‰, resulting in a maximal error (1σ) of ±0.4°C for isotopic temperatures obtained over this depth range. The 1σ standard deviation from replicate standard measurements (minimum of eight standards during each run) is routinely 0.07‰ for $\delta^{18}O_c$. Taking each of these uncertainties into account, the upper error estimate (1σ) associated with ACT is ±0.45°C. The combined maximum error on ACD is −10 m and +16 m, respectively (see supporting information Figure S1). The slightly larger uncertainties for our upper estimates originate from the fact that the variability in $\delta^{18}O_{sw}$ increases with proximity to the surface.

Of the four equations tested, only (1) and (2) produce plausible values for ACD and ACT. Equations (3) and (4) were unable to match the measured and calculated $\delta^{18}O_c$ for many site and routinely produced ACTs

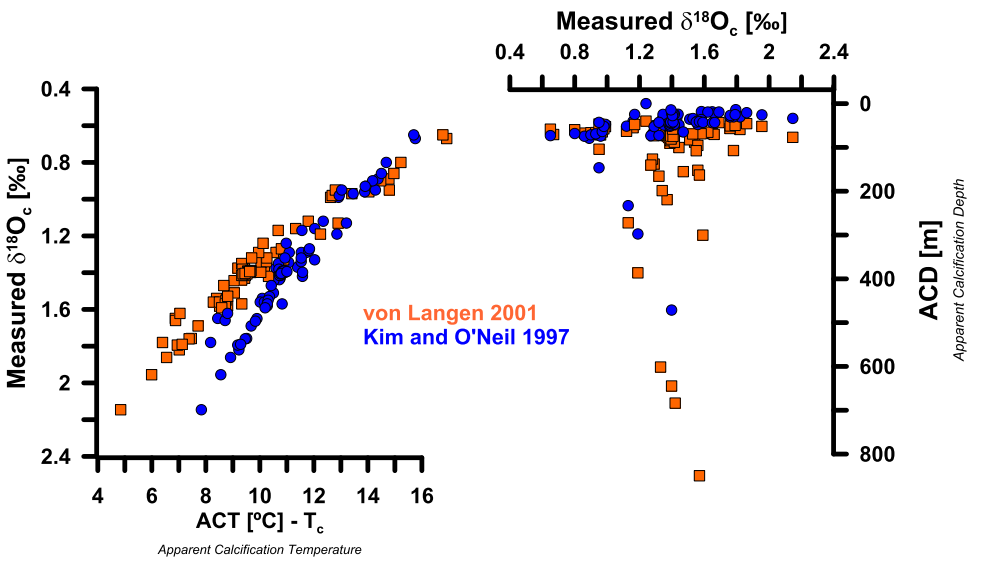

Figure 3. Sensitivity test for $\delta^{18}O$ paleotemperature equations. *N. incompta* $\delta^{18}O$ (‰) values are plotted against (left) ACT (°C) and (right) ACD (m) for data produced in this study and published previously (Elderfield & Ganssen 2000; Yu et al., 2008). Orange square symbols show ACT and ACD values using the equation from von Langen (2001) developed for *N. incompta*, while blue circles show ACT and ACD values obtained using the equation developed by Kim and O'Neil (1997).

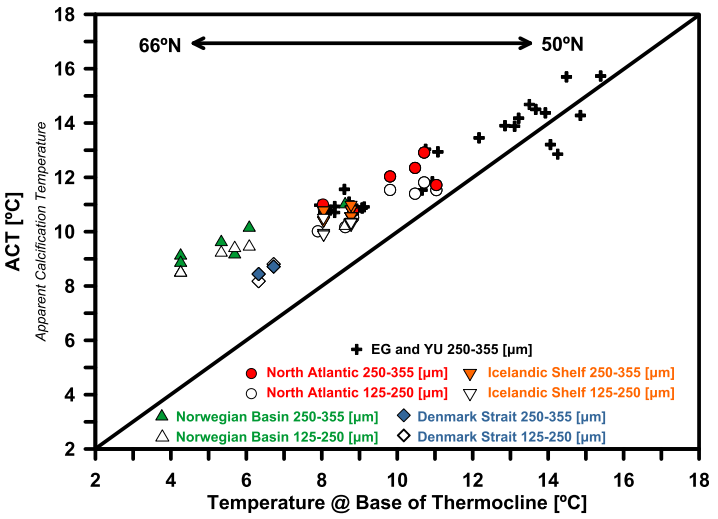

Figure 4. Isotopic temperature versus hydrographic temperature at the base of the seasonal thermocline for all sites. Isotopic temperatures were derived from all $\delta^{18}O_c$ values (including replicates; see Table 1). Sites from the Norwegian Basin are marked by green upward triangles, sites from the Denmark Strait in blue diamonds, sites from the subpolar North Atlantic in red circles, and sites from the Iceland Shelf in downward orange triangles. Samples previously measured by EG and YU are shown in black crosses. Fractions 150–255 μm are white while size fraction 255–355 μm is colored.

that are warmer than surface values, which resulted in negative ACD values. In many cases, ACD values calculated using equation (2) are unrealistically deep (below the seasonal thermocline), while equation (1) produces the most consistent ACD for all sites (average ACD = 44 ± 18 m; Figure 3). The Mg/Ca-temperature sensitivity is dependent on which $\delta^{18}O$ paleotemperature equation is selected. This is especially significant at lower temperatures (<12°C), where the measured $\delta^{18}O_c$-temperature relationship deviates between equations (1) and (2) (Figure 3). Although equation (2) was developed for *N. incompta*, we decided to proceed with equation (1) since calculated ACDs are more consistent for all sites included in this study. We suggest this result is due to equation (2) having been developed for Pacific *N. incompta* in a high temperature range (9–20°C), where (1) and (2) are not statistically different.

4.2. ACDs and ACTs

Assuming that $\delta^{18}O_c$ corresponds primarily to hydrographic parameters, rather than biologically induced vital effects, we record an average ACD of 41 ± 17 m (average ± SD) for large and 44 ± 16 m for small specimens. For all samples, the resulting ACTs range between 8.2 and 15.7 ± 0.45°C. When comparing ACT to the temperature at the base of the seasonal thermocline, we note that *N. incompta* tends to calcify just above the base of the seasonal thermocline. However, with increasing latitude, ACDs appear to decouple from the base of the seasonal thermocline toward shallower depths (Figure 4). The total range of isopycnal surfaces observed for all stations and replicate analyses spans σ_t = 26.2–27.2 (Figure 5). Therefore, compared to values reported for *N. pachyderma* (*s.*) (e.g., σ_t 27.7–27.8; Kozdon et al., 2009), *N. incompta* appears to be somewhat less partial to a distinct isopycnal surface, instead following latitudinal temperature distributions of the upper surface waters.

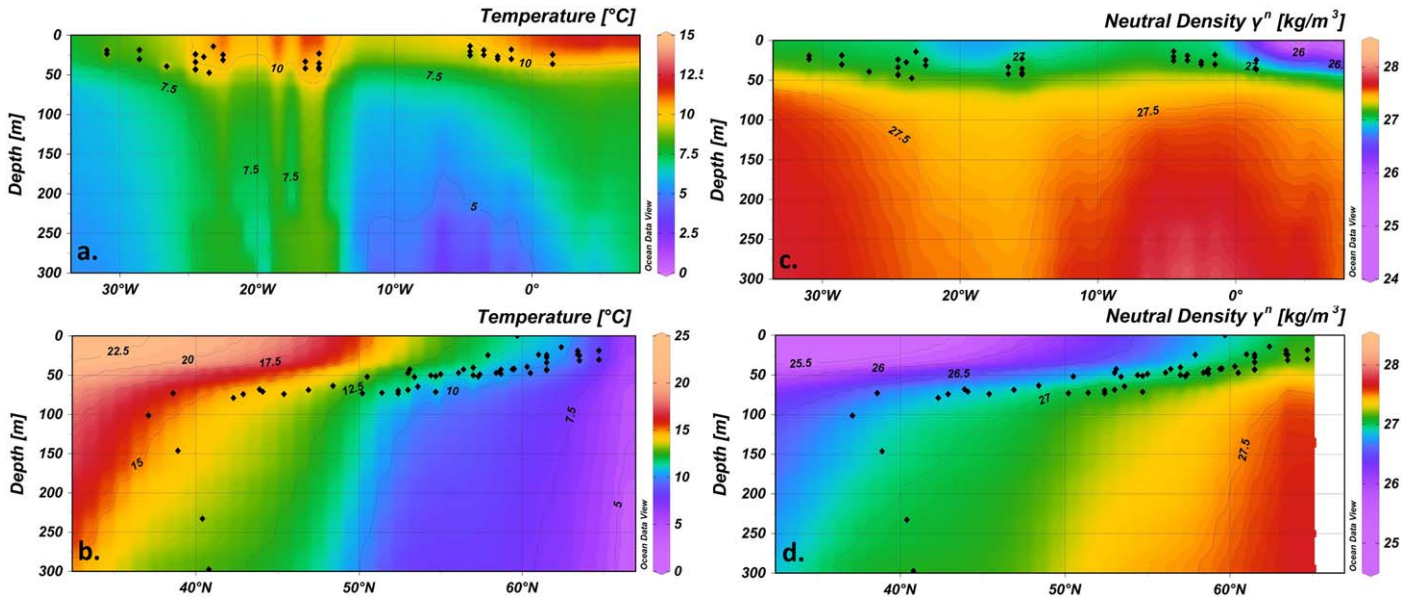

Figure 5. (Hydrography) Hydrographic sections produced with ODV (Schlitzer, 2002) using the WOA 09 (Antonov et al., 2010; Locarnini et al., 2010) seasonal data set for July to September. (a, c) Centered at 63.5°N and integrate seasonal data over a mean width of 750 km and (b, d) use a mean integration window of 1,500 km. Figures 5a and 5b show seasonal temperature distributions for their respective sections over the upper 300 m of surface waters, while Figures 5c and 5d show neutral density surfaces over same depths range. Black diamonds in all sections represent estimated calcification depths for each sample (including replicates) inferred from measured stable oxygen isotopes (see also section 4.1).

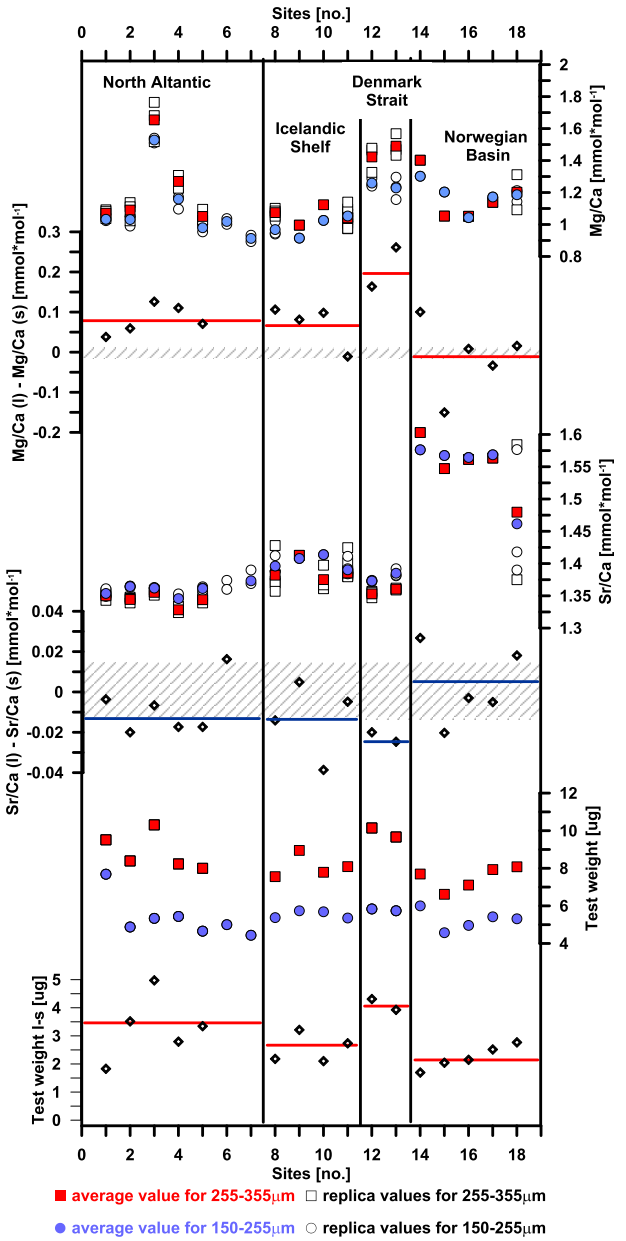

Figure 6. This plot shows an assessment of size differences on Mg/Ca, Sr/Ca, and test weight. Blue circles represent average values for size fractions 150–255 μm (s, small) and red squares represent average values for size fraction 255–355 μm (l, large). White circles (150–255 μm) and white squares (255–355 μm) show replica measurements for each site. The shaded areas illustrate the uncertainty associated with respective measurements (Mg/Ca = ±0.02 mmol mol^{-1}; Sr/Ca = ±0.015 mmol mol^{-1}). For sites from the Icelandic Shelf, ash-corrected values for Mg/Ca are shown (see Figure 4 for uncorrected values). The 18 sites are grouped according to region and then by increasing latitude. The mean weights for size fractions 150–255 and 255–355 μm is 5.47 and 8.75 μg, respectively.

4.3. Trace Element-to-Calcium Ratios

Mg/Ca values range between 0.89 and 2.55 mmol mol^{-1}. In keeping with an earlier study by Friedrich et al. (2012), we find that Mg/Ca values for *N. incompta* decrease with increasing test size so that consistently lower values are recorded in the smaller size fraction, with an average offset of 0.11 mmol mol^{-1} (±0.071; Figure 6). The relationship between Mg/Ca and calcification temperatures for our data set is shown in Figure 7 alongside previously published data from EG and YU and von Langen et al. (2005). There is considerable scatter throughout the data set. Notably, we observe large variations in values for samples collected from the Icelandic Shelf, Denmark Strait, Norwegian Basin, and MC 48, whereas all values from lower latitudes fall within the ranges observed previously by EG and YU. For values below 10°C, we observe a distinct departure from the typical Mg/Ca-temperature relationship, with increasing Mg/Ca values at lower temperatures. This effect is most pronounced in samples from the Denmark Strait region (e.g., MC78 and MC83) and from the Norwegian Basin (e.g., KN177-1). We also note that Mg/Ca values of samples from the vicinity of the Icelandic Shelf and from site MC48 are significantly higher than expected given their calcification temperatures.

To assess possible contamination of Mg/Ca values from clay or clay derivatives, we routinely measured Al and Fe. A regional analysis of Mg/Ca, Al/Ca, and Fe/Ca ratios for all sites reveals a significant relationship among these three elements for samples collected on or near the Icelandic Shelf, suggesting the possibility of volcanogenic silicate contamination in those samples. The slopes of the relationships are 0.43 (±0.06) for Mg/Ca versus Al/Ca and 0.40 (± 0.08) for Mg/Ca versus Fe/Ca, with both correlations having the same intercept within 95% CIs (regressions were calculated using values in mmol mol^{-1}, and a graph showing these relationships is provided in supporting information Figure S3). For the Denmark Strait and Norwegian Basin sites, Al/Ca and Fe/Ca values are relatively high (i.e., >100 μmol mol^{-1}), yet there is no consistent relationship with Mg/Ca, suggesting minimal Mg addition through postdepositional processes. Furthermore, we found no positive relationship between Al and Fe at these sites, confirming that these elements are derived from clay sources rather than fresh volcanic material (i.e., ash).

5. Discussion

In the following section, we evaluate the biological and environmental controls on the Mg/Ca-temperature relationship for *N. incompta*. First, we briefly discuss the observed differences in $\delta^{18}O_c$ and Mg/Ca values between two different test size fractions, 150–255 and 255–350 μm. We then provide a detailed assessment of the Mg/Ca-temperature relationship, which takes into account possible sources of Mg contamination (ash) and the effect of postdepositional dissolution, diagenesis, and, finally, the impact of seawater carbonate chemistry on the Mg/Ca signature.

5.1. Age of Samples

Care was taken to select foraminifera from the topmost sediments in multicores for geochemical analysis. While we cannot exclude the effects of bioturbation in areas of low sedimentation, we assume that this approach affords late Holocene foraminifera that can be paired with modern hydrographic data. This

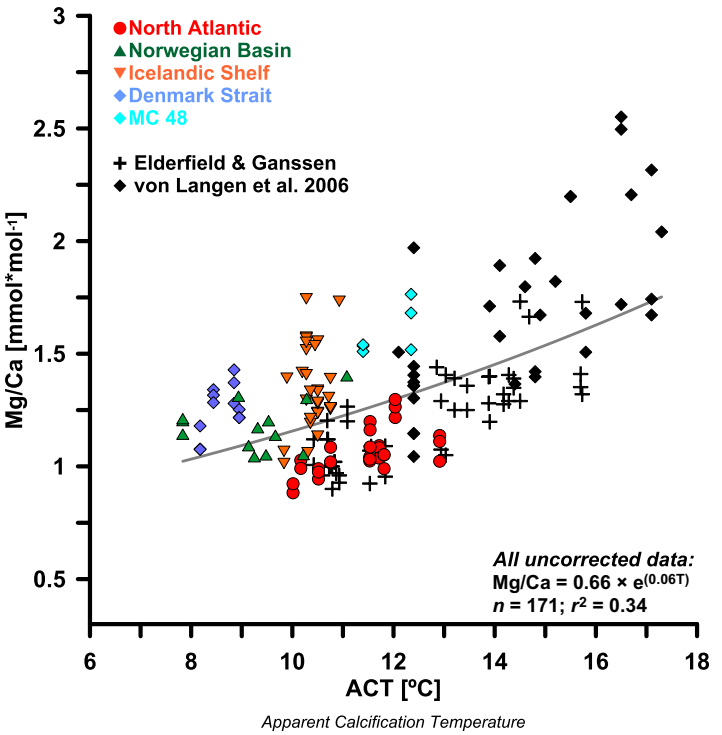

Figure 7. Plot showing uncorrected Mg/Ca values (including all replicates for all 18 sites and all size fractions) together with previously published data sets from EG, YU and von Langen et al. (2005) versus apparent calcification temperatures derived using $\delta^{18}O_c$ values. The resultant exponential Mg/Ca-temperature relationship including all data is weak and follows $Mg/Ca = 0.66 \times e^{(0.06T)}$ ($n = 171$; $r^2 = 0.34$).

assumption is supported by other core-top studies that generally yielded late Holocene calibrated AMS ^{14}C radiocarbon ages for the top centimeter of multicore tops (e.g., Marchitto et al., 2007; Simstich et al., 2003 and references therein). If, however, tests grew during significantly warmer (e.g., Holocene Thermal Maximum; 10,000–5,000 years ago) times, then we would expect this to be mirrored in oxygen isotopes values that were used to determine calcification temperatures. A key strength of the paired geochemical approach is that the thermal history is embedded similarly in different temperature proxies (Mg/Ca and $\delta^{18}O_c$), thereby resulting in a calibration that reflects the calcification conditions. The consistent ACDs of 41 ± 17 and 44 ± 16 m for large and small samples, respectively, and the tendency for ACTs to follow modern hydrographic profiles and latitudinal temperature distributions (Figures 3 and 5), both support the use of this approach.

5.2. Differences in $\delta^{18}O_c$ and Mg/Ca Values Between Two Size Classes

The difference in $\delta^{18}O_c$ values between larger and smaller test sizes translates into overall calcification temperatures that are 0.43 ± 0.35°C warmer for larger specimens. This being said, the observed offset in $\delta^{18}O_c$ between the 150–255 and 255–355 μm size fractions is small but significant, as they exceed the measurement errors associated with $\delta^{18}O_c$ measurements (i.e., the offsets are larger than $\pm 0.072‰$). However, when considering the errors derived for ACD and ACT (e.g., ± 16 m and ± 0.45°C), the offset is no longer significant. In the literature, possible origins for a size-dependent offset have been proposed and explained in relation to environmental factors (e.g., calcification depth) or biologically mediated processes, generally termed "vital effects" (Billups & Spero, 1995; Ezard et al., 2015). For non-photosymbiont-bearing species like *N. incompta*, vital effects may include the formation of an outer crust, growth (calcification) rate, and respiration (Simstich et al., 2003; Spero & Lea, 1996; Srinivasan & Kennett, 1974; Stangeew, 2001).

During gametogenesis, many planktonic foraminifera including non-symbiont-bearing species add an additional layer of calcite to their test as they sink through the water column prior to reproduction (Arikawa, 1983; Bé, 1980; Berberich, 1996; Hemleben et al., 1989). This additional calcite or crust is thought to introduce bias to the stable-isotopic signature, toward higher $\delta^{18}O$ and lower $\delta^{13}C$ values as this crust is precipitated in deeper, cooler, and nutrient-rich waters (Hemleben et al., 1989; Lohmann, 1995; Schiebel & Hemleben, 2005). However, Stangeew (2001) reported no correlation between temperature and the formation of an outer crust for *N. pachyderma* (*s*), while Sautter (1998) found no correlation between temperature and encrustation for species of the genus *Neogloboquadrina*. The absence of either a size effect in $\delta^{13}C$ (Figure 2) or a size-related relationship between $\delta^{18}O_c$ and $\delta^{13}C$ values in this study suggests that, for *N. incompta*, the formation of a secondary crust does not significantly influence either $\delta^{18}O_c$ or $\delta^{13}C$ values. These observations also reduce the likelihood that changes in calcification rate (through ontogeny; Berger et al., 1978; Ravelo & Fairbanks, 1995; Spero & Lea, 1996) or respiration (McConnaughey, 1989) influence the recorded isotopic values. The minimal response of the *N. incompta* growth rate to increasing temperatures relative to other planktonic foraminifera, and the fact that larger *N. pachyderma* (*s*) tests calcify more slowly with increasing temperatures (Lombard et al., 2009), provides additional support for our interpretation. Nonetheless, we acknowledge that there is a limited consensus about the influence of an outer crust on $\delta^{18}O_c$, $\delta^{13}C$, and temperature for species of the genus *Neogloboquadrina* and even less for *N. incompta* specifically.

Thus, in light of the available evidence, we favor the interpretation that larger specimens calcify in slightly warmer surface waters and smaller specimen in cooler upper thermocline waters, similar to reconstructions of habitat migration patterns for *Neogloboquadrina dutertrei* (Eggins et al., 2003). This interpretation also

aligns with known water-column distributions of most planktonic foraminifera, which stipulate that larger foraminifera tend to occupy warmer surface waters compared to smaller test sizes (e.g., Schiebel et al., 2001). We acknowledge that our analysis considers only two size fractions of large range, which makes it difficult to identify a significant size effect for ACD and ACT. Furthermore, the absence of a discernible size effect for $\delta^{13}C$ may also be due to the small gradient in $\delta^{13}C$ observed in the surface ocean. Nevertheless, our interpretation is consistent with observations of cultured *N. incompta* that record no significant relationship between $\delta^{18}O_c$ and $\delta^{13}C$ values (von Langen, 2001). For paleoceanographic applications, we would thus recommend the use of a narrow size fraction to reduce any size-related variability in ACTs.

Elderfield et al. (2002) hypothesized that increasing test size for both symbiont-bearing and non-symbiont-bearing species may be associated with increasing $\delta^{13}C$ and Mg/Ca but decreasing in Sr/Ca, due to variations in the distribution coefficients of Mg versus Sr at higher calcification rates. However, Friedrich et al. (2012) refute this hypothesis as they were unable to reproduce the relationship between Mg/Ca and $\delta^{13}C$ for symbiont-bearing or non-symbiont-bearing (e.g., *G. bulloides* and *N. incompta*) species. In addition, they argue that Mg/Ca-derived and $\delta^{18}O_c$-derived temperatures follow a 1:1 relationship and show a near proportionate temperature difference for small and large size classes. Similarly, we cannot identify a relationship between Mg/Ca and $\delta^{13}C$ for each size class, nor do we observe one between Sr/Ca and $\delta^{13}C$ (Figures 2 and 6).

The average difference in Mg/Ca values between larger and smaller test sizes is 0.065 mmol mol^{-1}. Using a Mg/Ca-temperature sensitivity of 10% per °C (see equation (5)), this offset translates into an overall temperature increase of 0.5–0.8°C for larger specimens (for temperatures of 8–13°C). This temperature differential agrees with ACT $\delta^{18}O_c$-based estimates, thereby supporting our interpretation that the size-specific offsets in Mg/Ca and $\delta^{18}O_c$ values reflect preferred depth habitats rather than biologically induced vital effects.

5.3. Sediment Contamination: Volcanic Ash

An analysis of Mg/Ca, Al/Ca, and Fe/Ca ratios for all sites reveals a significant relationship among these three elements for the Icelandic Shelf region (e.g., LCD-S1, LCD-S3, LCD-S6, and LCD-S7; Figure 8). Here volcanic ash/shards are the most likely contaminant since distinct brown and colorless glass shards and fragments of basaltic rock are present in these core-top samples (Figure 9). The positive correlation between Fe/Ca and Al/Ca suggests that both Fe and Al in the test reflect silicate contamination. The constancy of the molar Fe/Al value 0.89 ($\pm$0.07) suggests that the composition of the Al-silicate contaminant is uniform for all core tops (Figure 8). The uniform slopes and intercepts of the correlations between Al/Ca, Fe/Ca, and Mg/Ca are also consistent with a contaminant characterized by near-constant ratios of Al:Fe:Mg, such as volcanic Al-silicate debris. The positive Al/Ca intercept of 182 $\pm$ 41 further suggests that a small fraction of the Al might be associated with another secondary phase. Finally, the slope of the Fe-Al relationship is equivalent to an Al_2O_3-FeO weight ratio of $\sim$5:4, which is consistent with the composition of volcanic rocks from southern Iceland (Lackschewitz & Wallrabe-Adams, 1997; Oelkers & Gislason, 2001). We conclude, therefore, that the strong correlation of Mg to Fe and Al indicates that some of the observed Mg variability is not associated with primary test Mg, but instead reflects postdepositional contamination by volcanic phases.

Following Lea et al. (2005), we propose a correction scheme for our Icelandic Shelf samples. This approach assumes that not all of the Al in the samples, and the accompanying Mg, is test bound and therefore can be removed by subtraction. To test the validity of this approach, we analyzed multiple 400 μg aliquots/splits for both size fractions in core tops from three sites on the Icelandic Shelf. Depending on availability of *N. incompta*, we were then able to replicate the analysis between 3 and 9 times (Figure 8). If the correction scheme is valid, all repeated samples should end up with the same Mg/Ca value regardless of the level of contamination. Indeed, the correction scheme produces highly consistent results regardless of Al or Fe values. The 2σ standard deviation for corrected splits is low for all sites and size fractions analyzed, and the resultant temperatures are within the error of isotopic ACTs (see Figure 8 and Table 2). It is noteworthy that this range in variability is comparable to the natural variability observed in noncontaminated samples from the North Atlantic data set. We also note that the correction scheme produces similar values for both size fractions. A further advantage of this correction scheme is that it can be applied to

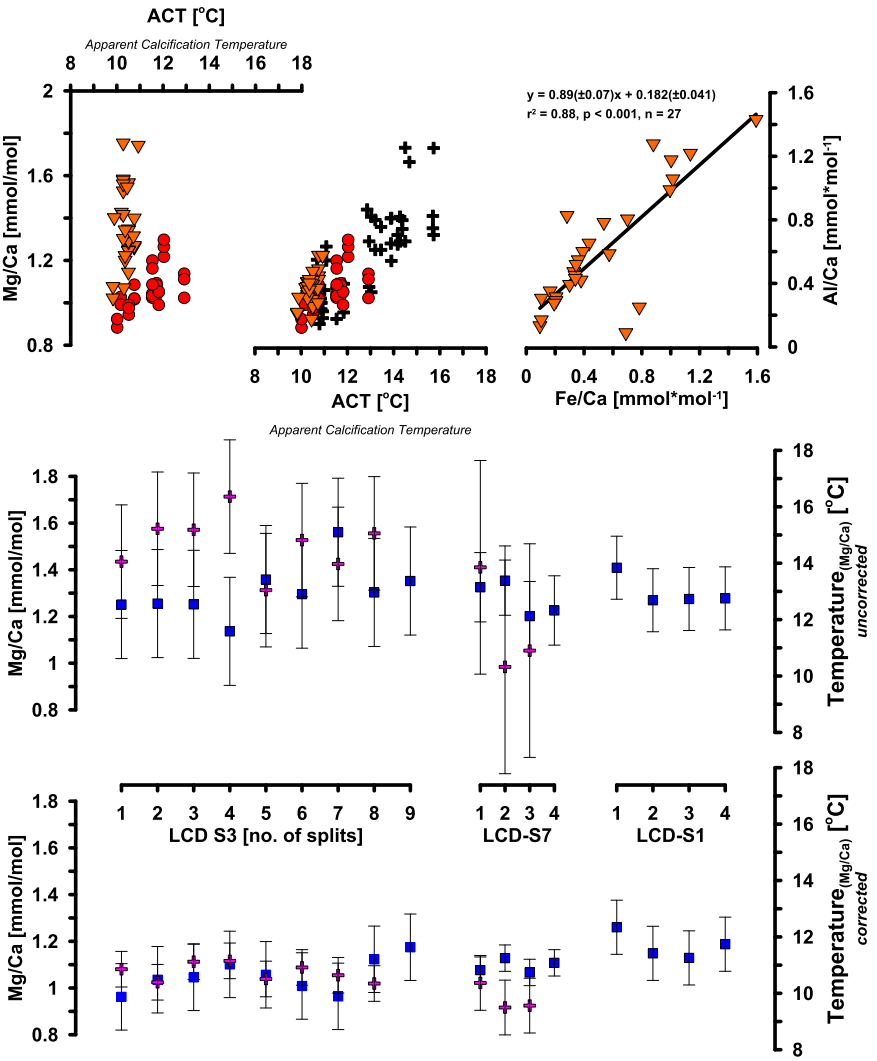

Figure 8. Assessment of ash correction scheme. (top row) Uncorrected samples from the Icelandic Shelf (downward orange triangles) together with (red circles) and (top left) E&G (black crosses) versus ACT. In the central Icelandic Shelf, samples are corrected for ash contamination and the top right graph illustrates the relationship between Fe/Ca and Al/Ca for samples analyzed. (middle row) All uncorrected Mg/Ca values and their respective temperatures for each of the three sites (LCD-S1, -S3, and -S7). Also shown are the 2σ standard deviations for each measurement. Pink crosses represent replicate samples from the 150–255 μm size fraction and blue squares represent replicate samples from the 255–355 μm size fraction. (bottom row) We applied the proposed correction scheme to the same samples and the 2σ standard deviations for each sample highlights the reproducibility of the approach.

paleoceanographic down-core reconstructions, since Al and Fe are often routinely measured alongside Mg in foraminifera tests.

5.4. Postdepositional Dissolution

Previous investigations show that calcite dissolution occurring in undersaturated ($\Delta CO_3^{2-} > 0$ μmol kg^{-1}, $\Omega > 1$) bottom waters causes the Mg/Ca ratios of foraminiferal tests to decrease (Brown & Elderfield, 1996; Dekens et al., 2002; Johnstone et al., 2011; Regenberg et al., 2006). Dissolution of calcite can occur within the water column, at the water-sediment interface, and within the sediments. To investigate the possible effects of postdepositional dissolution on *N. incompta* in the current data set, we plotted bottom water temperature (WOA09) against bottom water ΔCO_3^{2-} for all sites (Figure 10). Calculation of ΔCO_3^{2-} for each core site was accomplished by subtracting the carbonate-ion concentration [CO_3^{2-}] at saturation (Jansen et al., 2002) from in situ [CO_3^{2-}] measurements. For computing in situ [CO_3^{2-}] values, we used the program

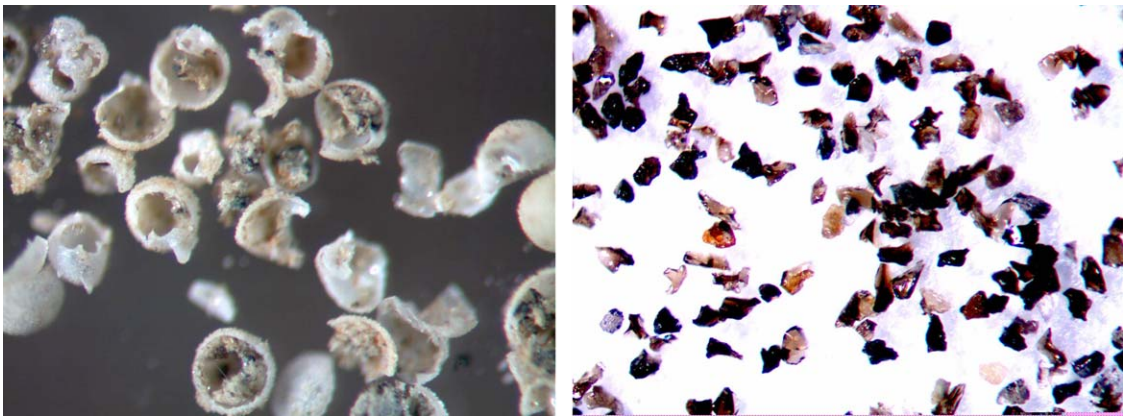

Figure 9. Images of crushed foraminifera showing dark specks (left) of ash in and around test wall and (right) of ash particles from Iceland samples.

CO2sys.xls (Pelletier et al., 2007), with K1 and K2 refitted by Dickson and Millero (1987) and KSO_4 after Dickson (1990).

Only one site falls below the critical threshold of 21.3 ± 6.6 μmol kg^{-1}, identified by Regenberg et al. (2014) as the value at which Mg/Ca is significantly influenced by dissolution (KN177-1 MC31; 5.54 μmol kg^{-1}). Mg/Ca ratios from MC31 are, however, higher than expected based on the calcification temperature. To further assess the potential impact of bottom water ΔCO_3^{2-} on foraminiferal Mg/Ca, we plotted ΔCO_3^{2-} against test weight (Figure 10; De Villiers, 2005; Rosenthal et al., 2000; Rosenthal & Lohmann, 2002). While we acknowledge that the method used to determine test weights is limited by the accuracy of the scale, we find no relationship between decreasing test weight and decreasing ΔCO_3^{2-} for either size fraction (150–255 and 255–355 μm), suggesting that bottom water dissolution is unlikely to have altered the Mg content of tests used in this study.

5.5. Carbonate Overgrowths/Diagenesis

Differences in pore water chemistry associated with variable sedimentation rates and background lithology, in particular calcium carbonate content, can influence foraminiferal Mg/Ca ratios through sediment diagenetic processes. For example, lower bottom water oxygen levels could potentially lead to remobilization of free metals and postdepositional recrystallization of manganese-rich carbonate phases, which might explain higher-than-expected Mg/Ca values (Boyle, 1983). If low-oxygen conditions prevailed in sediments, we would predict a higher concentration of redox-sensitive elements, such as manganese, leading to higher Mn/Ca values recorded in foraminifera. Therefore, if overgrowths were an issue for any of the core sites, we would expect lower bottom water oxygen levels to correlate with higher Mg/Ca and Mn/Ca values. For all sites in our study, bottom water oxygen levels range from 4.44 to 7.04 mL L^{-1} and all Mn/Ca values fall below 100 μmol mol^{-1}. We note that, for oxygen levels below 5.5 mL L^{-1}, Mn/Ca values increase with decreasing bottom water oxygen content, especially at site MC45. Nonetheless, Mg/Ca values for this site fall within the expected spectrum. Therefore, we assume that Mg/Ca values at MC45 are unaffected by

Table 2
Summary of Ash Correction Scheme (See Also Figure 8)

			$Mg/Ca_{(Av)}$ (mmol mol^{-1})	2σ			$Temp_{(Av)}$ (°C)	2σ			
Site	Size (μm)	No. of splits	*Uncorrected*		*Corrected*		*Uncorrected*		*Corrected*		$ACT_{(iso)}$
LCD-S1	255–355	4	1.29	0.13	1.15	0.10	13.00	1.12	11.69	0.96	10.75
	150–255	1	1.06	*na*	1.03	*na*	10.84	*na*	10.46	*na*	10.30
LCD-S3	255–355	9	1.29	0.23	1.04	0.11	13.00	1.92	10.62	1.18	10.50
	150–255	8	1.51	0.27	1.05	0.06	14.71	2.01	10.74	0.63	10.28
LCD-S7	255–355	4	1.26	0.14	1.07	0.06	12.74	1.23	10.97	0.47	10.36
	150–255	3	1.16	0.41	0.97	0.09	11.69	3.79	9.81	0.97	9.83

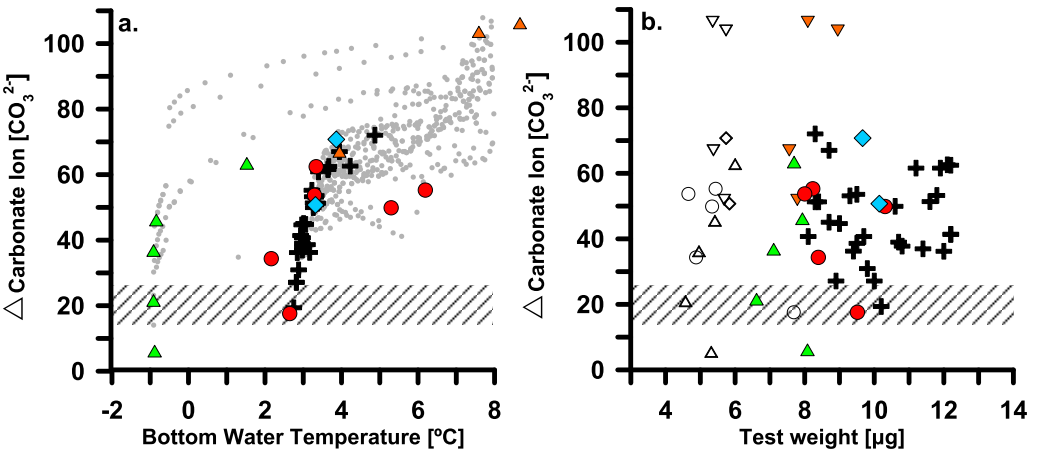

Figure 10. Assessment of bottom water Δ carbonate-ion concentration on foraminiferal test weight. (a) Delta carbonate-ion concentration against bottom water temperatures (WOA 09) for all water-column profiles for all stations (gray dots). We further highlighted bottom water values for the Norwegian Basin (green upward triangles), Denmark Strait (blue diamonds), North Atlantic (red circles), Icelandic Shelf (downward orange triangles), and for the EG and YU data set (black crosses). (b) We plotted ΔCO_3^{2-} against test weight for each sample. The colored symbols represent weights for the 255–355 μm size fractions and the empty symbols represent weights for the 150–255 μm size fraction. Finally, we inserted the critical threshold of 21.3 ± 0.6 μmol kg^{-1} (hashed area) identified by Regenberg et al. (2014) below which Mg/Ca values may be significantly influenced by dissolution.

manganese contamination, as no apparent relationship between Mn/Ca versus Mg/Ca or Mg/Ca versus bottom water oxygen exists (Figure 11).

Foraminiferal tests collected from calcareous sediments of carbonate mounts might be contaminated with high-Mg abiotic overgrowths acquired on the seafloor. Inorganic calcite precipitated in laboratory studies contains about an order of magnitude more Mg than planktonic foraminiferal calcite (Baker et al., 1982; Katz, 1973; Mucci, 1987; Mucci & Morse, 1983). Thus, only a limited amount of overgrowth remaining after Mg-cleaning procedures would be sufficient to raise Mg/Ca values. Recent investigations in the Mediterranean Sea, using trace metal analysis in conjunction with SEM, suggest that high-Mg overgrowths on foraminifera collected from supersaturated bottom waters may be responsible for elevated Mg/Ca values (Boussetta et al., 2011; Hoogakker et al., 2009; Reuning et al., 2005; van Raden et al., 2011). Although not all diagenetic inorganic calcite contains high Mg as the chemical signature is largely a function of the calcium carbonate type within the sediment column. MC 48 from this study was collected from a carbonate mount (Rockall Bank) and we record elevated Mg/Ca values (average 36.5%) for both size fractions from this site.

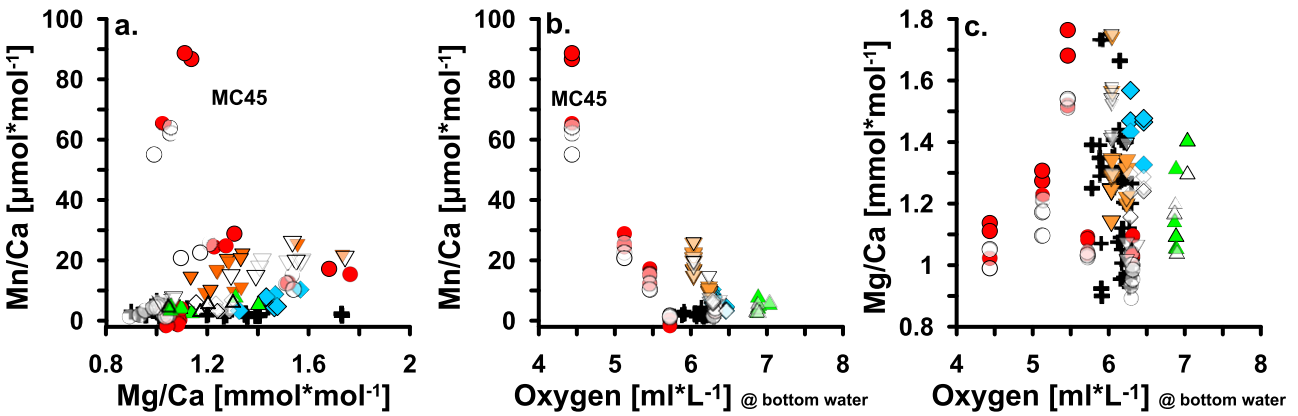

Figure 11. Assessment of (a) Mn/Ca values against Mg/Ca, (b) Mn/Ca against bottom water oxygen, and (c) Mg/Ca against bottom water oxygen. Samples from the Norwegian Basin are shown as green upward triangles, from the Denmark Strait as blue diamonds, from the North Atlantic as red circles, from the Icelandic Shelf (uncorrected for ash contamination) as orange downward triangles, and the EG and YU data set is shown as black crosses. Bottom water oxygen content was obtained from World Ocean Atlas 2009 (Garcia et al., 2010).

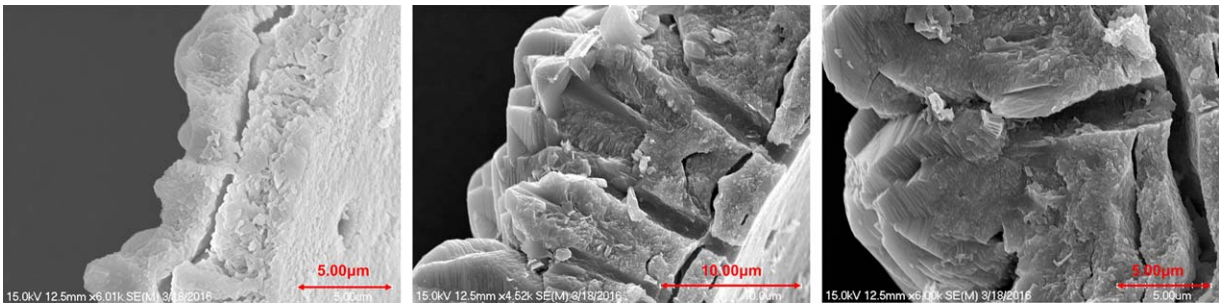

Figure 12. Assessment of inorganic overgrowth on MC48. SEM images of *N. incompta*. (left) Control image from MC36 (open ocean). (middle and right) MC48 collected in vicinity of a carbonate mount.

Sr/Ca values cannot be used as an indicator for carbonate overgrowth as previously suggested (e.g., Regenberg et al., 2007) because the Rockall Bank site is characterized by hardgrounds, where the porewater Sr/Ca cannot build up sufficiently to form diagenetic calcite with high Sr/Ca values. Accordingly, Sr/Ca values for MC48 are no different than for other sites included in this study (1.2–1.7 mmol mol^{-1}). To investigate the potential of diagenesis in samples taken from MC48, we prepared several individuals for SEM analyses. The images (Figure 12) provide evidence for the addition of inorganically precipitated calcite rhombohedrons on the exterior test walls of specimens. More detailed sampling techniques should be used to validate the presence of inorganic calcite and whether this translates to variable Mg/Ca phase. Consequently, we exclude MC 48 from the remainder of the discussion, as Mg/Ca are likely biased by high-Mg overgrowth carbonate phases.

5.6. Seawater Carbonate Chemistry

Planktonic foraminifera culturing experiments reveal a significant relationship between carbonate chemistry (pH and [CO_3^{2-}]) and Mg/Ca in several species, resulting in a general increase of Mg/Ca values with decreasing [CO_3^{2-}] values (Evans et al., 2016; Kisakürek et al., 2008; Lea et al., 1999; Russell et al., 2004). This pattern implies that absolute Mg/Ca-derived temperatures may be systematically biased to higher values when ocean pH or [CO_3^{2-}] was significantly lower than typical modern seawater values. While a carbonate-ion concentration correction is routinely applied to some benthic foraminifera species (Lear et al., 2010; Sosdian & Rosenthal, 2009; Yu et al., 2010), there remains uncertainty on how (or if) such a correction should be applied to planktonic foraminifera.

In *N. pachyderma* (*s.*), the potential effect of low [CO_3^{2-}] on Mg/Ca values was previously hypothesized (Meland et al., 2006) and further discussed in Hendry et al. (2009). In the latter study, authors used B/Ca-derived [CO_3^{2-}] values applying equations developed in Yu et al. (2007) for *Globorotalia inflata* to estimate the impact of [CO_3^{2-}] on *N. pachyderma* (*s*) Mg/Ca values. Since [CO_3^{2-}] and temperature covary in Margarite Bay, Antarctica, they were not able to isolate the impact of changing [CO_3^{2-}] on Mg/Ca as is possible in culturing studies (Evans et al., 2016; Kisakürek et al., 2008; Lea et al., 1999; Russell et al., 2004). As shown in a recent compilation study by Evans et al. (2016), this change in sensitivity is most adequately expressed by a power rather than a linear function and appears to be valid for multiple planktonic foraminifera species. In practice, this means that when [CO_3^{2-}] and temperature covary, the influence of carbonate-ion concentration is negligible at high [CO_3^{2-}] values (or values $>$ 200 μmol kg^{-1}) and temperature dominates Mg/Ca ratios. However, at low [CO_3^{2-}] values (e.g., $<$200 μmol kg^{-1}), the influence of temperature on Mg/Ca is compromised by a strong carbonate-ion concentration effect.

To estimate the influence of seawater [CO_3^{2-}] on Mg/Ca values for our calibration data set, we propose to isolate the contribution of [CO_3^{2-}] on measured Mg/Ca values. Unfortunately, explicit culture experiments evaluating the role of [CO_3^{2-}] on Mg/Ca in *N. incompta* have yet to be performed. Therefore, we propose to derive the Mg/Ca sensitivity to [CO_3^{2-}] using water-column data for temperature and carbonate-ion concentration, following a similar approach as described by Evans et al. (2016). First, we normalized measured Mg/Ca values against predicted Mg/Ca values (e.g., Mg/Ca$_{[T]}$) by deriving a Mg/Ca-temperature equation for all samples included in this study with [CO_3^{2-}] values exceeding 200 μmol kg^{-1}, as we consider this subset to be negligibly influenced by [CO_3^{2-}] (see Evans et al. (2016)). This affords the following equation:

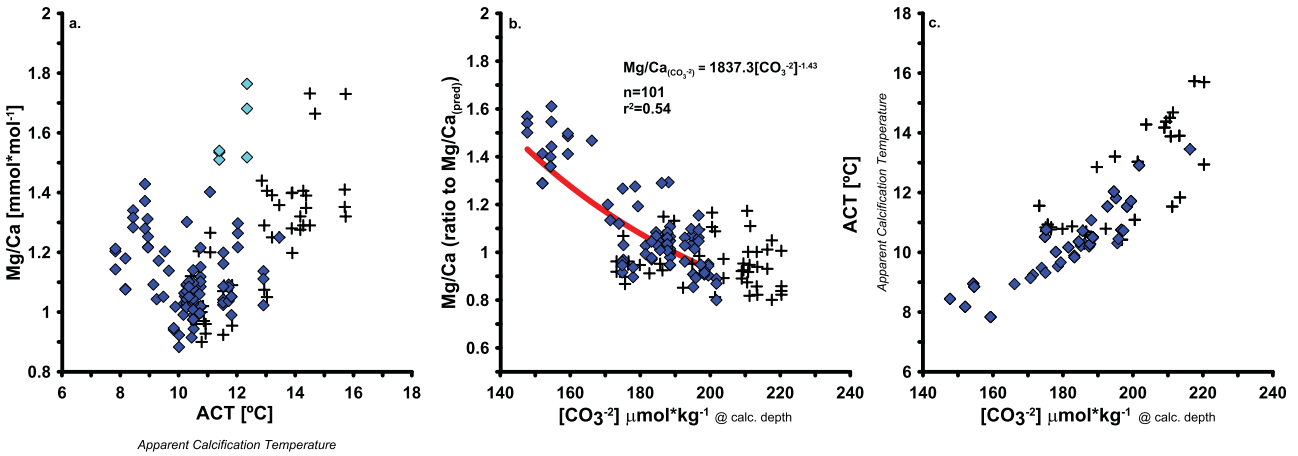

Figure 13. Assessment of the carbonate-ion concentration effect on Mg/Ca values measured on *N. incompta*. All new samples from this study are shown in blue diamonds (MC48 in cyan) and the EG and YU data set is shown as black crosses. (a) The distribution of measured Mg/Ca values against ACT. (b) The normalized Mg/Ca values against water-column $[CO_3^{2-}]$ values. The power function shown applies to $[CO_3^{2-}]$ values below 200 μmol kg^{-1} as this subset is likely to be influenced by $[CO_3^{2-}]$ (see Evans et al., 2016). (c) The relationship between temperature and $[CO_3^{2-}]$ in the water column at apparent calcification depth.

$$Mg/Ca_{[T]} = 0.4e^{(0.09ACT)} \left(n = 127,\ r^2 = 0.72\right) \tag{5}$$

Similar to Evans et al. (2016), we then derived the relationship between Mg/Ca ratios ($Mg/Ca_{[meas]}/Mg/Ca_{[pred]}$) and water-column carbonate-ion concentrations (Figure 13), which provided us with the following relationship for sites where $[CO_3^{2-}] < 200$ μmol kg^{-1}:

$$Mg/Ca_{[CO_3]} = 1837.3\left[CO_3^{2-}\right]^{-1.433} \left(n = 101,\ r^2 = 0.54\right) \tag{6}$$

Finally, we corrected our data set by dividing $Mg/Ca_{[meas]}$ by equation (6) to yield the following correction equation for the calibration data set (Figure 14):

$$\begin{aligned} Mg/Ca_{[meas]} &= Mg/Ca_{[T]} \times Mg/Ca_{[CO3]} \\ &= \left(0.4e^{(0.09ACT)}\right)\left(1837.3\left[CO_3^{2-}\right]^{-1.433}\right. \end{aligned} \tag{7}$$

The final calibration equation, which includes all corrected values and the culture data set from von Langen (2006), is

$$Mg/Ca = 0.40e^{(0.09ACT)};\ \left(n = 173,\ r^2 = 0.77\right) \tag{8}$$

We note that equation (6) is steeper than equations presented in Evans et al. (2016) and propose that the discrepancy between equations can be explained as a nonlinear response of $[CO_3^{2-}]$ on Mg incorporation at various ambient temperatures. We would predict that at lower temperatures the $[CO_3^{2-}]$ ion effect would be greater than at higher temperatures. This hypothesis needs to be tested in culturing studies, however several lines of evidence support this interpretation. First, a significant carbonate-ion concentration effect for polar and subpolar foraminifera that calcify at low temperatures has previously been hypothesised, and is evident in several core-top-based calibration data sets (e.g., Hendry et al., 2009; Meland et al., 2006). Second, to our knowledge none of the core-top-based Mg/Ca calibrations for tropical and subtropical foraminifera indicate the presence of an $[CO_3^{2-}]$ effect on Mg/Ca values at their low temperature range (Anand et al., 2003; Cléroux et al., 2008; Dekens et al., 2002; Elderfield & Ganssen, 2000; Regenberg et al., 2009). This may be because the $[CO_3^{2-}]$ effect is smaller at higher temperatures in the tropics and subtropics, and that at these latitudes, temperature exerts the dominant control on Mg/Ca even at low $[CO_3^{2-}]$ values. The combination of low temperatures and low $[CO_3^{2-}]$ at subpolar latitudes may therefore result in a much stronger response to low $[CO_3^{2-}]$ values, which would be evident by a steeper slope. Furthermore such low $[CO_3^{2-}]$ simulated in the lab do not exist within the preferred habitat of common tropical species. This limits our ability to quantify the $[CO_3^{2-}]$ ion effect on Mg/Ca from core-top sediments of those genera. To estimate the uncertainties for derived temperatures associated with this correction scheme, we combined errors

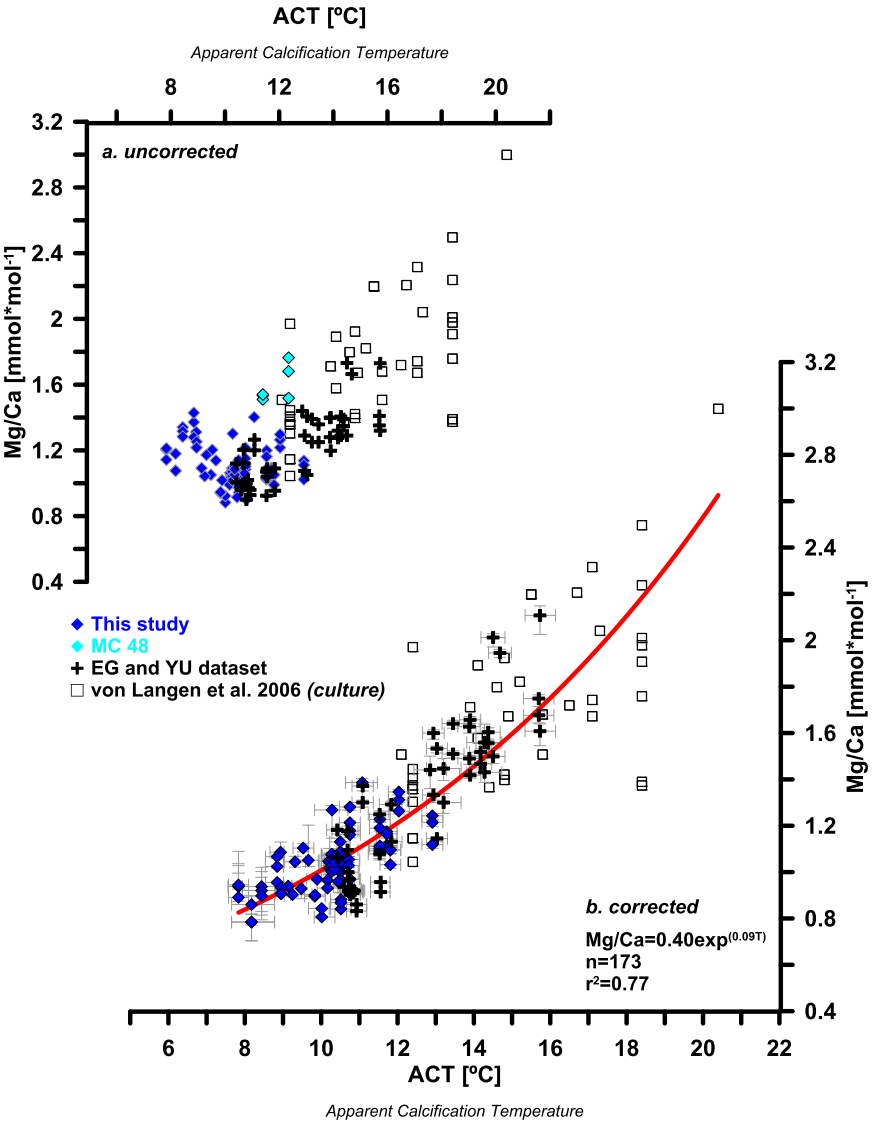

Figure 14. Mg/Ca values corrected for seawater carbonate-ion concentration. (a) The uncorrected data set and (b) the corrected values and the calibration equation applied to all samples used in this study and the culture set from von Langen et al. (2005).

associated with equation (6), linking Mg/Ca and $[CO_3^{2-}]$ ($\pm$0.118 mmol mol^{-1} (1σ SD)) to uncertainties associated with our calibration equation (5) ($\pm$0.138 mmol mol^{-1} (1σ SD)), and uncertainties associated with estimating calcification temperatures ($\pm$0.45°C (1σ SD)). Since all uncertainties are independent from each other, we applied simple additive error propagation calculations for a final estimate of uncertainties associated with predicted temperatures using the proposed correction scheme: $\pm$2.78°C (1σ SD). We stress that these large uncertainties may originate from the limited data available to estimate the relationship between $Mg/Ca_{[CO_3]}$ for values $<$ 200 μmol kg^{-1}, and that future additions to this data set and/or species-specific relationships for *N. incompta* will undoubtedly reduce the uncertainties with this approach.

5.7. Paleoceanographic Implications

The implication of the $[CO_3^{2-}]$ control on Mg/Ca values is that the community may have underestimated cooling episodes during past glacial periods, and possibly also during interglacial cold events (e.g., during present and penultimate interglacials), using Mg/Ca-derived paleotemperature reconstructions. This underestimation is potentially greatest at high latitudes, where $[CO_3^{2-}]$ values are often below 200 μmol kg^{-1}. To

demonstrate the impact of $[CO_3^{2-}]$ on Mg/Ca for records spanning Pleistocene glacial-interglacial time scales, and to test the validity of our correction scheme, we applied our approach to published down-core data sets. In order to account for seawater $[CO_3^{2-}]$ changes, an independent $[CO_3^{2-}]$ proxy is required. A similar multiproxy approach is employed to disentangle bottom water ocean temperature and $[CO_3^{2-}]$ in benthic foraminifera using B/Ca (Yu & Elderfield, 2008) and Li/Ca (Lear et al., 2010) to estimate past $[CO_3^{2-}]$. Boron/calcium (B/Ca) in planktonic foraminifera is proposed to reflect ambient seawater carbonate chemistry (Allen & Hönisch, 2012; Howes et al., 2017) and can be routinely measured alongside Mg/Ca, making it an ideal proxy to evaluate the influence of past seawater $[CO_3^{2-}]$ changes. A fundamental understanding of noncarbonate controls (e.g., salinity, phosphate, and B_{sw}) influencing the B/Ca proxy continues to evolve and should also be considered when applying this correction scheme. Despite these uncertainties core-top calibration studies determined similar B/Ca-$[CO_3^{2-}]$ sensitivity in the Atlantic Ocean with *N. pachyderma* (*s*) (Yu et al., 2013) and, more recently, in the Pacific Ocean with *N. incompta* (Krupinski et al., 2017). However, to our knowledge, there are no paired Mg/Ca and B/Ca paleoceanographic reconstructions currently available for *N. incompta* with which to test our proposed correction scheme. Instead, we apply our correction to two previously published records that discussed Mg/Ca-derived temperatures and B/Ca measured on *N. pachyderma* (*s*) (Irvalı et al., 2012; Yu et al., 2013). Considering that the impact of carbonate-ion concentration on Mg/Ca at low temperatures appears to be valid for multiple planktonic foraminifera species (Evans et al., 2016), we argue that this approach is appropriate. Furthermore, consistent $[CO_3^{2-}]$ sensitivities on B/Ca are observed in both species (Krupinski et al., 2017; Yu et al., 2013). However, the magnitude of change resulting from the correction needs to be confirmed with species-specific measurements in culture experiments.

The first down-core application is from the South Iceland Rise (Yu et al., 2013) and covers approximately 7,000 (ka), from 11 to 18 ka, during the last deglaciation. The chronology for the core was provided by Thornalley et al. (2010). For trace metal analysis, approximately 100–200 *N. pachyderma* (*s*) tests were picked from the 150–250 μm size fraction and cleaned according to the Mg-cleaning protocol (Barker et al., 2003). The data set for the second application was collected from the Eirik Drift, South Greenland (Irvalı et al., 2012). The record covers ~20 ka, from 120 to 140 ka, and spans Termination II into the last interglacial period. For trace metal analysis, ~40 *N. pachyderma* (*s*) were selected from the 150–250 μm size fraction and measured at the Department of Marine and Coastal Sciences, Rutgers University, using a Thermo Finnigan Element XR (SF-ICP-MS) and the same protocols employed in this study.

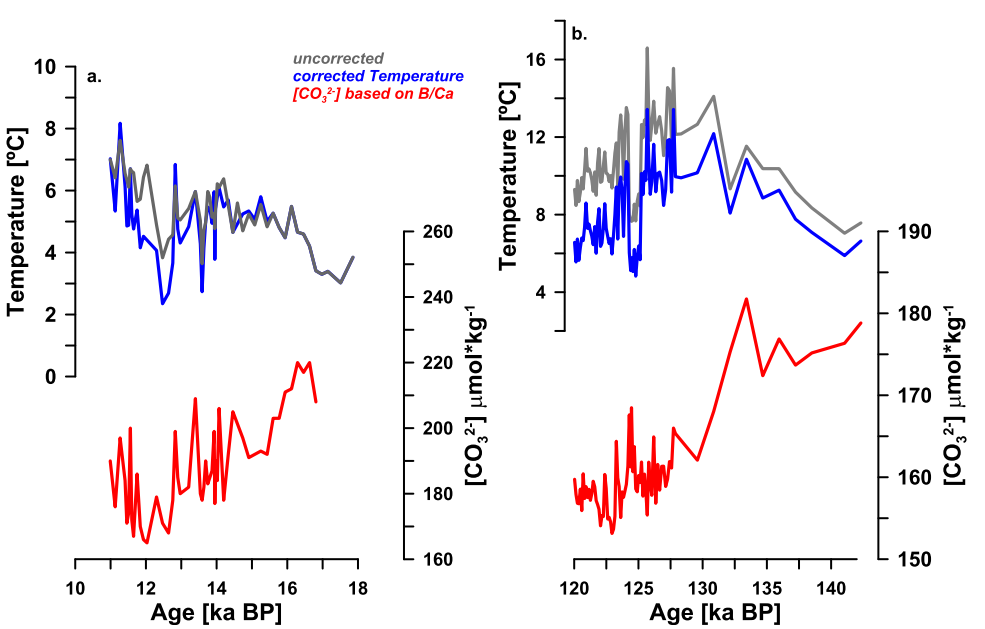

Figure 15. Down-core applications of carbonate-ion concentration correction scheme showing corrected Mg/Ca values for sea water carbonate ion. (a) Data published in Yu et al. (2013) and (b) data published in Irvalı et al. (2012).

We calculate past [CO_3^{2-}] values using paired B/Ca values, following relationships established by Yu et al. (2013) for *N. pachyderma* (*s*), and then applied our correction scheme as described above. The results are shown in Figure 15. Both records show that estimated cooling for abrupt cold events during MIS 5e and the Younger Dryas may have been underestimated by over 2°C. Moreover, the magnitude of SST change over glacial-deglacial transitions may also have been underestimated due to the sensitivity of Mg/Ca to low [CO_3^{2-}]. Likewise, both the trend and high-frequency variability in subpolar North Atlantic SSTs may have been underestimated by as much as 2 and 4°C, respectively, during the last interglacial. The latter is particularly significant as the corrected data document rapid interglacial climate change, for example, at 125.24 ka, when SSTs dropped by >5°C within 100 years and remained low for a millennium. The short centennial duration of these events, combined with the confounding influence of [CO_3^{2-}] on Mg/Ca-temperature reconstructions, may have reduced our ability to identify the true magnitude of interglacial climate changes. Applying corrected proxy calibrations in ultra-high sedimentation rate settings, where bioturbative smoothing is minimized, hints that the view of interglacial climate as "stable" may still be presumptuous. Ultimately, species-specific equations for *N. incompta* are needed in order to provide more quantifiable estimates of the effect of [CO_3^{2-}] on Mg/Ca for the glacial ocean with acceptable error envelopes.

6. Conclusions

We show that a careful analysis of multiple trace elements and stable isotope geochemistry can provide valuable new tools to assess the validity of Mg/Ca as a proxy for surface ocean temperature. The multidimensional assessment of the data set presented here provides a means not only to constrain and identify biological, environmental, and external processes affecting the Mg/Ca signature of planktonic foraminifera, but also to correct for them. Our results highlight the importance for multiple trace element-to-calcium ratios including, Al, Fe, Mn, U, Sr, and B/Ca to estimate paleotemperatures more accurately. Our assessment of the environmental controls on Mg/Ca in *N. incompta* reveals the following:

1. Size-specific offsets in Mg/Ca and $\delta^{18}O_c$ values are consistent with habitat migration patterns throughout the life cycle of *N. incompta* and indicate that larger specimens calcify in warmer surface waters relative to smaller specimens, which appear to favor the upper thermocline. The observed offset between size fractions is 0.43 ± 0.35°C for calcification temperatures reconstructed from $\delta^{18}O_c$ values and between 0.5 and 0.8°C for calcification temperatures reconstructed from Mg/Ca values.
2. The contamination of volcanic ash within the test lattice can be effectively removed by subtraction following the method outlined by Lea et al. (2005). The 2σ standard deviation for ash-corrected samples is less than ±0.1 mmol mol^{-1}.
3. The addition of high-Mg abiotic overgrowths leads to higher-than-expected Mg/Ca values. We identified evidence for the addition of inorganically precipitated euhedral calcite on the exterior test walls of specimens collected from MC48, a site located close to a carbonate mount near the Rockall Bank. To differentiate inorganic overgrowth from ontogenetic calcite phases, microsampling techniques could be used to investigate the chemical composition and structure of these sample specimen further (Eggins et al., 2003; Jonkers et al., 2016; Sadekov et al., 2005).
4. The seawater carbonate chemistry at calcification depth proves to have a significant impact on the Mg/Ca-temperature relationship. For values > 200 μmol kg^{-1}, we find that temperature exerts the dominant control on Mg/Ca values, while at values < 200 μmol kg^{-1}, the carbonate-ion concentration of seawater increases the uptake of Mg into the test lattice, thereby resulting in higher-than-expected Mg/Ca values at low temperatures. Our proposed correction scheme successfully removes the carbonate-ion concentration effect from the calibration data set and affords new possibilities to reconstruct the full magnitude of past ocean cooling.

Acknowledgments
We thank R. Kozdon, D. Evans, and two anonymous reviewers for insightful discussions and constructive revisions of this manuscript. The data set generated and/or analyzed during the current study are available at www.pangaea.de. All authors declare no competing financial interests. A.M. and Y.R. conceived the project. A.M., T.B., and Y.R. interpreted the record. A.M. and T.B. wrote the manuscript text. J.W. provided stable-isotopic data set. U.N., H.K., and N.I. contributed B/Ca data and contributed to the discussion on the paleoceanographic implications of the proposed correction scheme. A.M. acknowledges the Postdoctoral Fellowship Program in Earth, Ocean, and Atmospheric Sciences at Rutgers University for funding.

References

Allen, K. A., & Hönisch, B. (2012). The planktic foraminiferal B/Ca proxy for seawater carbonate chemistry: A critical evaluation. *Earth and Planetary Science Letters, 345–348*, 203–211. https://doi.org/10.1016/j.epsl.2012.06.012

Anand, P., Elderfield, H., & Conte, M. H. (2003). Calibration of Mg/Ca thermometry in planktonic foraminifera from a sediment trap time series. *Paleoceanography, 18*(2), 1050. https://doi.org/10.1029/2002PA000846

Antonov, J. I., Seidov, D., Boyer, T. P., Locarnini, R. A., Mishonov, A. V., Garcia, H. E., . . . Johnson, D. R. (2010). World Ocean Atlas 2009, volume 2: Salinity. In S. Levitus (Ed.), *NOAA atlas NESDIS 69*. Washington, DC: U.S. Government Printing Office.

Arikawa, R. (1983). Distribution and taxonomy of globigerina pachyderma (Ehrenberg) off the Sanriku coast, northeast Honshu, Japan, The science reports of the Tohoku University. Second series. *Geology*, *53*(2), 103-A120.
Babila, T. L., Rosenthal, Y., & Conte, M. H. (2014). Evaluation of the biogeochemical controls on B/Ca of Globigerinoides ruber white from the Oceanic Flux Program, Bermuda. *Earth and Planetary Science Letters*, *404*, 67–76.
Baker, P. A., Gieskes, J. M., & Elderfield, H. (1982). Diagenesis of carbonates in deep-sea sediments—Evidence from SR/CA ratios and interstitial dissolved SR2+ data. *Journal of Sedimentary Research*, *52*(1), 71–82.
Barker, S., Cacho, I., Benway, H., & Tachikawa, K. (2005). Planktonic foraminiferal Mg/Ca as a proxy for past oceanic temperatures: A methodological overview and data compilation for the Last Glacial Maximum. *Quaternary Science Reviews*, *24*(7), 821–834.
Barker, S., Greaves, M., & Elderfield, H. (2003). A study of cleaning procedures used for foraminiferal Mg/Ca paleothermometry. *Geochemistry Geophysics Geosystems*, *4*(9), 8407. https://doi.org/10.1029/2003GC000559
Bé, A. (1980). Gametogenic calcification in a spinose planktonic foraminifer, Globigerinoides sacculifer (Brady). *Marine Micropaleontology*, *5*, 283–310.
Bemis, B. E., Spero, H. J., & Thunell, R. C. (2002). Using species-specific paleotemperature equations with foraminifera: A case study in the Southern California Bight. *Marine Micropaleontology*, *46*(3), 405–430.
Berberich, D. (1996). *Die planktische Foraminifere Neogloboquadrina pachyderma (Ehrenberg) im Weddellmeer, Antarktis* [*The planktonic foraminifere Neogloboquadrina pachyderma (Ehrenberg) in the Weddell Sea, Antarctica*] (Berichte zur Polarforschung [Rep. Polar Res.] 195).
Berger, W. H., Killingley, J. S., & Vincent, E. (1978). Stable isotopes in deep-sea carbonates: Box core ERDC-92, west equatorial Pacific. *Oceanologica Acta*, *1*, 203–216.
Billups, K., & Spero, H. J. (1995). Relationship between shell size, thickness and stable isotopes in individual planktonic foraminifera from two Equatorial Atlantic cores. *Journal of Foraminiferal Researchh*, *25*(1), 24–37.
Boussetta, S., Bassinot, F., Sabbatini, A., Caillon, N., Nouet, J., Kallel, N., . . . Labeyrie, L. (2011). Diagenetic Mg-rich calcite in Mediterranean sediments: Quantification and impact on foraminiferal Mg/Ca thermometry. *Marine Geology*, *280*(1), 195–204.
Boyle, E. A. (1983). Chemical accumulation variations under the Peru Current during the past 130,000 years. *Journal of Geophysical Research*, *88*(C12), 7667–7680.
Boyle, E. A., & Keigwin, L. D. (1985). Comparion of Atlantic and Pacific paleochemical records for the last 215,000 years: Changes in deep ocean circulation and chemical inventories. *Earth and Planetary Science Letters*, *76*, 135–150.
Brown, S. J., & Elderfield, H. (1996). Variations in Mg/Ca and Sr/Ca ratios of planktonic foraminifera caused by postdepositional dissolution: Evidence of shallow Mg-dependent dissolution. *Paleoceanography*, *11*(5), 543–551.
Chapman, M. R. (2010). Seasonal production patterns of planktonic foraminifera in the NE Atlantic Ocean: Implications for paleotemperature and hydrographic reconstructions. *Paleoceanography*, *25*, PA1101. https://doi.org/10.1029/2008PA001708
Cléroux, C., Cortijo, E., Anand, P., Labeyrie, L., Bassinot, F., Caillon, N., & Duplessy, J.-C. (2008). Mg/Ca and Sr/Ca ratios in planktonic foraminifera: Proxies for upper water column temperature reconstruction. *Paleoceanography*, *23*, PA3214. https://doi.org/10.1029/2007PA001505
Darling, K. F., Kucera, M., Kroon, D., & Wade, C. M. (2006). A resolution for the coiling direction paradox in *Neogloboquadrina pachyderma*. *Paleoceanography*, *21*, PA2011. https://doi.org/10.1029/2005PA001189
Dekens, P. S., Lea, D. W., Pak, D. K., & Spero, H. J. (2002). Core top calibration of Mg/Ca in tropical foraminifera: Refining paleotemperature estimation. *Geochemistry Geophysics Geosystems*, *3*(4), 1022. https://doi.org/10.1029/2001GC000200
De Villiers, S. (2005). Foraminiferal shell-weight evidence for sedimentary calcite dissolution above the lysocline. *Deep Sea Research, Part I: Oceanographic Research Papers*, *52*(5), 671–680.
Dickson, A. (1990). Thermodynamics of the dissociation of boric acid in synthetic seawater from 273.15 to 318.15 K. *Deep Sea Research, Part A: Oceanographic Research Papers*, *37*(5), 755–766.
Dickson, A., & Millero, F. J. (1987). A comparison of the equilibrium constants for the dissociation of carbonic acid in seawater media. *Deep Sea Research, Part A: Oceanographic Research Papers*, *34*(10), 1733–1743.
Eggins, S., De Deckker, P., & Marshall, J. (2003). Mg/Ca variation in planktonic foraminifera tests: Implications for reconstructing palaeoseawater temperature and habitat migration. *Earth and Planetary Science Letters*, *212*(3), 291–306.
Elderfield, H., & Ganssen, G. (2000). Past temperature and $\delta^{18}O$ of surface ocean waters inferred from Mg/Ca ratios. *Nature*, *405*, 442–445.
Elderfield, H., Vautravers, M., & Cooper, M. (2002). The relationship between shell size and Mg/Ca, Sr/Ca, $\delta^{18}O$, and $\delta^{13}C$ of species of planktonic foraminifera. *Geochemistry, Geophysics, Geosystems*, *3*(8). https://doi.org/10.1029/2001GC000194
Evans, D., Wade, B. S., Henehan, M., Erez, J., & Müller, W. (2016). Revisiting carbonate chemistry controls on planktic foraminifera Mg/Ca: Implications for sea surface temperature and hydrology shifts over the Paleocene–Eocene Thermal Maximum and Eocene–Oligocene transition. *Climate of the Past*, *12*(4), 819–835.
Ezard, T. H., Edgar, K. M., & Hull, P. M. (2015). Environmental and biological controls on size-specific $\delta^{13}C$ and $\delta^{18}O$ in recent planktonic foraminifera. *Paleoceanography*, *30*, 151–173. https://doi.org/10.1002/2014PA002735
Fairbanks, R., & Wiebe, P. (1980). Foraminifera and chlorophyll maximum: Vertical distribution, seasonal succession, and paleoceanographic significance. *Science*, *209*(4464), 1524–1526. https://doi.org/10.1126/science.209.4464.1524
Friedman, I., & O'Neil, J. R. (1977). *Data of geochemistry: Compilation of stable isotope fractionation factors of geochemical interest*. Washington, DC: U.S. Government Printing Office.
Friedrich, O., Schiebel, R., Wilson, P. A., Weldeab, S., Beer, C. J., Cooper, M. J., & Fiebig, J. (2012). Influence of test size, water depth, and ecology on Mg/Ca, Sr/Ca, $\delta^{18}O$ and $\delta^{13}C$ in nine modern species of planktic foraminifers. *Earth and Planetary Science Letters*, *319*, 133–145.
Garcia, H., Locarnini, R., Boyer, T., Antonov, J., Baranova, O., Zweng, M., & Johnson, D. (2010). World Ocean Atlas 2009, volume 3: Dissolved oxygen, apparent oxygen utilization, and oxygen saturation. In S. Levitus (Ed.), *NOAA atlas NESDIS 70*. Washington, DC: U.S. Government Printing Office.
Hemleben, C., Spindler, M., & Anderson, O. R. (1989). *Modern planktonic foraminifera* (363 pp.). New York, NY: Springer.
Hendry, K. R., Rickaby, R. E., Meredith, M. P., & Elderfield, H. (2009). Controls on stable isotope and trace metal uptake in *Neogloboquadrina pachyderma* (sinistral) from an Antarctic sea-ice environment. *Earth and Planetary Science Letters*, *278*(1), 67–77.
Hoogakker, B. A., Klinkhammer, G. P., Elderfield, H., Rohling, E. J., & Hayward, C. (2009). Mg/Ca paleothermometry in high salinity environments. *Earth and Planetary Science Letters*, *284*(3), 583–589.
Hopkins, T. S. (1991). The GIN Sea—A synthesis of its physical oceanography and literature review 1972–1985. *Earth Science Reviews*, *30*(3), 175–318.
Howes, E. L., Kaczmarek, K., Raitzsch, M., Mewes, A., Bijma, N., Horn, I., . . . Bijma, J. (2017). Decoupled carbonate chemistry controls on the incorporation of boron into Orbulina universa. *Biogeosciences*, *14*(2), 415.
Irvalı, N., Ninnemann, U. S., Galaasen, E. V., Rosenthal, Y., Kroon, D., Oppo, D. W., . . . Kissel, C. (2012). Rapid switches in subpolar North Atlantic hydrography and climate during the Last Interglacial (MIS 5e). *Paleoceanography*, *27*, PA2207. https://doi.org/10.1029/2011PA002244

Jansen, H., Zeebe, R. E., & Wolf-Gladrow, D. A. (2002). Modeling the dissolution of settling $CaCO_3$ in the ocean. *Global Biogeochemical Cycles*, *16*(2). https://doi.org/10.1029/2000GB001279

Johnstone, H. J., Lee, W., & Schulz, M. (2016). Effect of preservation state of planktonic foraminifera tests on the decrease in Mg/Ca due to reductive cleaning and on sample loss during cleaning. *Chemical Geology*, *420*, 23–36.

Johnstone, H. J., Yu, J., Elderfield, H., & Schulz, M. (2011). Improving temperature estimates derived from Mg/Ca of planktonic foraminifera using X-ray computed tomography–based dissolution index, XDX. *Paleoceanography*, *26*, PA1215. https://doi.org/10.1029/2009PA001902

Jonkers, L., Buse, B., Brummer, G.-J. A., & Hall, I. R. (2016). Chamber formation leads to Mg/Ca banding in the planktonic foraminifer *Neogloboquadrina pachyderma*. *Earth and Planetary Science Letters*, *451*, 177–184.

Katz, A. (1973). The interaction of magnesium with calcite during crystal growth at 25–90°C and one atmosphere. *Geochimica et Cosmochimica Acta*, *37*(6), 1563IN31579–15615781586.

Kim, S.-T., & O'Neil, J. R. (1997). Equilibrium and nonequilibrium oxygen isotope effects in synthetic carbonates. *Geochimica et Cosmochimica Acta*, *61*(16), 3461–3475.

Kisakürek, B., Eisenhauer, A., Böhm, F., Garbe-Schönberg, D., & Erez, J. (2008). Controls on shell Mg/Ca and Sr/Ca in cultured planktonic foraminiferan, Globigerinoides ruber (white). *Earth and Planetary Science Letters*, *273*(3–4), 260–269.

Kohfeld, K. E., Fairbanks, R. G., Smith, S. L., & Walsh, I. D. (1996). *Neogloboquadrina pachyderma* (sinistral coiling) as paleoceanographic tracers in polar oceans: Evidence from Northeast Water Polynya plankton tows, sediment traps, and surface sediments. *Paleoceanography*, *11*(6), 679–699.

Kozdon, R., Eisenhauer, A., Weinelt, M., Meland, M. Y., & Nürnberg, D. (2009). Reassessing Mg/Ca temperature calibrations of *Neogloboquadrina pachyderma* (sinistral) using paired $\delta^{44/40}$Ca and Mg/Ca measurements. *Geochemistry, Geophysics, Geosystems*, *10*, Q03005. https://doi.org/10.1029/2008GC002169

Krauss, W. (1986). The North Atlantic Current. *Journal of Geophysical Research*, *91*(C4), 5061–5074.

Krauss, W. (1995). Currents and mixing in the Irminger Sea and in the Iceland Basin. *Journal of Geophysical Research*, *100*(C6), 10851–10871. https://doi.org/10.1029/95JC00423

Krupinski, N. B. Q., Russell, A. D., Pak, D. K., & Paytan, A. (2017). Core-top calibration of B/Ca in Pacific Ocean *Neogloboquadrina incompta* and *Globigerina bulloides* as a surface water carbonate system proxy. *Earth and Planetary Science Letters*, *466*, 139–151.

Kuroyanagi, A., & Kawahata, H. (2004). Vertical distribution of living planktonic foraminifera in the seas around Japan. *Marine Micropaleontology*, *53*(1–2), 173–196. https://doi.org/10.1016/j.marmicro.2004.06.001

Lackschewitz, K. S., & Wallrabe-Adams, H.-J. (1997). Composition and origin of volcanic ash zones in Late Quaternary sediments from the Reykjanes Ridge: Evidence for ash fallout and ice-rafting. *Marine Geology*, *136*(3–4), 209–224.

Lea, D., Mashiotta, T. A., & Spero, H. J. (1999). Controls on magnesium and strontium uptake in planktonic foraminifera determined by live culturing. *Geochimica et Cosmochimica Acta*, *63*(16), 2369–2379.

Lea, D., Martin, P. A., Pak, D. K., & Spero, H. J. (2002). Reconstructing a 350ky history of sea level using planktonic Mg/Ca and oxygen isotope records from a Cocos Ridge core. *Quaternary Science Reviews*, *21*(1), 283–293.

Lea, D., Pak, D., & Paradis, G. (2005). Influence of volcanic shards on foraminiferal Mg/Ca in a core from the Galápagos region. *Geochemistry, Geophysics, Geosystems*, *6*, Q11P04. https://doi.org/10.1029/2005GC000970

Lear, C., Elderfield, H., & Wilson, P. (2000). Cenozoic deep-sea temperatures and global ice volumes from Mg/Ca in benthic foraminiferal calcite. *Science*, *287*(5451), 269–272.

Lear, C., Mawbey, E. M., & Rosenthal, Y. (2010). Cenozoic benthic foraminiferal Mg/Ca and Li/Ca records: Toward unlocking temperatures and saturation states. *Paleoceanography*, *25*, PA4215. https://doi.org/10.1029/2009PA001880

LeGrande, A. N., & Schmidt, G. A. (2006). Global gridded data set of the oxygen isotopic composition in seawater. *Geophysical Research Letters*, *33*, L12604. https://doi.org/10.1029/2006GL026011

Locarnini, R. A., Mishonov, A. V., Antonov, J. I., Boyer, T. P., Garcia, H. E., Baranova, O. K., . . . Johnson, D. R. (2010). World Ocean Atlas 2009, volume 1: Temperature. In S. Levitus (Ed.), *NOAA atlas NESDIS 68*. Washington, DC: U.S. Government Printing Office.

Lohmann, G. P. (1995). A model for variation in the chemistry of planktonic foraminifera due to secondary calcification and selectiv dissolution. *Paleoceanography*, *10*(3), 445–457.

Lombard, F., Labeyrie, L., Michel, E., Spero, H. J., & Lea, D. W. (2009). Modelling the temperature dependent growth rates of planktic foraminifera. *Marine Micropaleontology*, *70*(1), 1–7.

Mackensen, A., Sejrup, H. P., & Jansen, E. (1985). The distribution of living benthic foraminifera on the continental slope and rise off southwest Norway. *Marine Micropaleontology*, *9*, 275–306.

Marchitto, T. M., Bryan, S. P., Curry, W. B., & McCorkle, D. C. (2007). Mg/Ca temperature calibration for the benthic foraminifer *Cibicidoides pachyderma*. *Paleoceanography*, *22*, PA1203. https://doi.org/10.1029/2006PA001287.

McConnaughey, T. (1989). C^{13} and O^{18} isotopic disequilibrium in biological carbonates: I. Patterns. *Geochimica et Cosmochimica Acta*, *53*, 151–162.

Meland, M. Y., Jansen, E., Elderfield, H., Dokken, T. M., Olsen, A., & Bellerby, R. G. (2006). Mg/Ca ratios in the planktonic foraminifer *Neogloboquadrina pachyderma* (sinistral) in the northern North Atlantic/Nordic Seas. *Geochemistry, Geophysics, Geosystems*, *7*, Q06P14. https://doi.org/10.1029/2005GC001078

Mucci, A. (1987). Influence of temperature on the composition of magnesian calcite overgrowths precipitated from seawater. *Geochimica et Cosmochimica Acta*, *51*(7), 1977–1984.

Mucci, A., & Morse, J. W. (1983). The incorporation of Mg^{2+} and Sr^{2+} into calcite overgrowths: Influences of growth rate and solution composition. *Geochimica et Cosmochimica Acta*, *47*(2), 217–233.

O'Brien, T., Conkright, M., Boyer, T., Antonov, J., Baranova, O., Garcia, H., . . . Murphy, P. (2002). World Ocean Database 2001. Volume 7, Temporal distribution of chlorophyll and plankton data. In S. Levitus (Ed.), *NOAA atlas NESDIS 48*. Washington, DC: U.S. Government Printing Office.

Oelkers, E. H., & Gislason, S. R. (2001). The mechanism, rates and consequences of basaltic glass dissolution: I. An experimental study of the dissolution rates of basaltic glass as a function of aqueous Al, Si and oxalic acid concentration at 25°C and pH = 3 and 11. *Geochimica et Cosmochimica Acta*, *65*(21), 3671–3681.

O'Neil, J. R., Clayton, R. N., & Mayeda, T. K. (1969). Oxygen isotope fractionation in divalent metal carbonates. *The Journal of Chemical Physics*, *51*(12), 5547–5558.

Ortiz, J. D., Mix, A. C., & Collier, R. W. (1995). Environmental control of living symbiotic and asymbiotic foraminifera of the California Current. *Paleoceanography*, *10*(6), 987–1009.

Pak, D. K., Lea, D. W., & Kennett, J. P. (2004). Seasonal and interannual variation in Santa Barbara Basin water temperatures observed in sediment trap foraminiferal Mg/Ca. *Geochemistry, Geophysics, Geosystems*, *5*, Q12008. https://doi.org/10.1029/2004GC000760

Pattiaratchi, C. B., Micallef, S., Aiken, J., Osborne, M., Collins, M., & Williams, R. (1989). Chlorophyll variability at Ocean Weather Station Lima (57°N, 20°W). In J. S. Ryland & P. A. Tyler (Eds.), *Reproduction, genetics and distributions of marine organisms: 23rd European Marine Biology Symposium*. Swansea, UK: Olsen & Olsen.

Pelletier, G., Lewis, E., & Wallace, D. (2007). *CO2Sys. xls: A calculator for the CO2 system in seawater for Microsoft excel/VBA*. Olympia, WA: Washington State Department of Ecology.

Ravelo, A., & Fairbanks, R. (1995). Carbon isotopic fractionation in multiple species of planktonic foraminifera from core-tops in the tropical Atlantic. *Oceanographic Literature Review*, *10*(42), 854.

Regenberg, M., Nürnberg, D., Schönfeld, J., & Reichart, G.-J. (2007). Early diagenetic overprint in Caribbean sediment cores and its effect on the geochemical composition of planktonic foraminifera. *Biogeosciences*, *4*(6), 957–973.

Regenberg, M., Nürnberg, D., Steph, S., Groeneveld, J., Garbe-Schönberg, D., Tiedemann, R., & Dullo, W. C. (2006). Assessing the effect of dissolution on planktonic foraminiferal Mg/Ca ratios: Evidence from Caribbean core tops. *Geochemistry, Geophysics, Geosystems*, *7*, Q07P15. https://doi.org/10.1029/2005GC001019

Regenberg, M., Regenberg, A., Garbe-Schönberg, D., & Lea, D. W. (2014). Global dissolution effects on planktonic foraminiferal Mg/Ca ratios controlled by the calcite-saturation state of bottom waters. *Paleoceanography*, *29*, 127–142. https://doi.org/10.1002/2013PA002492

Regenberg, M., Steph, S., Nürnberg, D., Tiedemann, R., & Garbe-Schönberg, D. (2009). Calibrating Mg/Ca ratios of multiple planktonic foraminiferal species with δ^{18}O-calcification temperatures: Paleothermometry for the upper water column. *Earth and Planetary Science Letters*, *278*(3), 324–336. https://doi.org/10.1016/j.epsl.2008.12.019

Reuning, L., Reijmer, J. J., Betzler, C., Swart, P., & Bauch, T. (2005). The use of paleoceanographic proxies in carbonate periplatform settings—Opportunities and pitfalls. *Sedimentary Geology*, *175*(1), 131–152.

Rosenthal, Y., Boyle, E. A., & Slowey, N. (1997). Temperature control on the incorporation of magnesium, strontium, fluorine, and cadmium into benthic foraminiferal shells from Little Bahama Bank: Prospects for thermocline paleoceanography. *Geochimica et Cosmochimica Acta*, *61*(17), 3633–3643.

Rosenthal, Y., Dahan, M., & Shemesh, A. (2000). Southern Ocean contribution to glacial-interglacial changes of atmospheric pCO_2: An assessment of carbon isotope record in diatoms. *Paleoceanography*, *15*(1), 65–75.

Rosenthal, Y., Field, M. P., & Sherrell, R. M. (1999). Precise determination of element/calcium ratios in calcareous samples using sector field inductively coupled plasma mass spectrometry. *Analytical Chemistry*, *71*(15), 3248–3253. https://doi.org/10.1021/ac981410x

Rosenthal, Y., & Lohmann, G. P. (2002). Accurate estimation of sea surface temperatures using dissolution-corrected calibrations for Mg/Ca paleothermometry. *Paleoceanography*, *17*(3), 1044. https://doi.org/10.1029/2001PA000749

Rosenthal, Y., Perron-Cashman, S., Lear, C. H., Bard, E., Barker, S., Billups, K., . . . Dwyer, G. S. (2004). Interlaboratory comparison study of Mg/Ca and Sr/Ca measurements in planktonic foraminifera for paleoceanographic research. *Geochemistry, Geophysics, Geosystems*, *5*, Q04D09. https://doi.org/10.1029/2003GC000650

Russell, A. D., Hönisch, B., Spero, H. J., & Lea, D. W. (2004). Effects of seawater carbonate ion concentration and temperature on shell U, Mg, and Sr in cultured planktonic foraminifera. *Geochimica et Cosmochimica Acta*, *68*(21), 4347–4361.

Sadekov, A. Y., Eggins, S. M., & De Deckker, P. (2005). Characterization of Mg/Ca distributions in planktonic foraminifera species by electron microprobe mapping. *Geochemistry, Geophysics, Geosystems*, *6*, Q12P06. https://doi.org/10.1029/2005GC000973

Sautter, L. R. (1998). Morphologic and stable isotopic variability within the planktic foraminiferal genus Neogloboquadrina. *Journal of Foraminiferal Research*, *28*(3), 220–232.

Sautter, L. R., & Sancetta, C. (1992). Seasonal associations of phytoplankton and planktic foraminifera in an upwelling region and their contribution to the seafloor. *Marine Micropaleontology*, *18*(4), 263–278.

Sautter, L. R., & Thunell, R. C. (1989). Seasonal succession of planktonic foraminifera; results from a four-year time-series sediment trap experiment in the Northeast Pacific. *The Journal of Foraminiferal Research*, *19*(4), 253–267.

Schiebel, R., & Hemleben, C. (2005). Modern planktic foraminifera. *Paläontologische Zeitschrift*, *79*(1), 135–148.

Schiebel, R., Waniek, J., Bork, M., & Hemleben, C. (2001). Planktic foraminiferal production stimulated by chlorophyll redistribution and entrainment of nutrients. *Deep Sea Research, Part I: Oceanographic Research Papers*, *48*(3), 721–740.

Schlitzer, R. (2002). Interactive analysis and visualization of geoscience data with Ocean Data View. *Computers & Geosciences*, *28*(10), 1211–1218. https://doi.org/10.1016/S0098-3004(02)00040-7

Shackleton, N. (1974). Attainment of isotopic equilibrium between ocean water and the benthonic foraminifera genus Uvigerina: Isotopic changes in the ocean during the last glacial. *Colloques Internationaux. Centre National De La Recherche Scientifique*, *219*, 203–209.

Simstich, J., Sarnthein, M., & Erlenkeuser, H. (2003). Paired δ^{18}O signals of *Neogloboquadrina pachyderma* (s) and *Turborotalita quinqueloba* show thermal stratification structure in Nordic Seas. *Marine Micropaleontology*, *48*(1), 107–125.

Sosdian, S., & Rosenthal, Y. (2009). Deep-sea temperature and ice volume changes across the Pliocene-Pleistocene climate transitions. *Science*, *325*(5938), 306–310. https://doi.org/10.1126/science.1169938

Spero, H. J., & Lea, D. W. (1996). Experimental determination of stable isotope variability in *Globigerina bulloides*: Implications for paleoceanographic reconstructions. *Marine Micropaleontology*, *28*, 231–246.

Srinivasan, M., & Kennett, J. (1974). Secondary calcification of the planktonic foraminifer *Neogloboquadrina pachyderma* as a climatic index. *Science*, *186*(4164), 630–632.

Stangeew, E. (2001). *Distribution and isotopic composition of living planktonic foraminifera N. pachyderma (sinistral) and T. quinqueloba in the high latitude North Atlantic*. Kiel, Germany: Christian-Albrechts Universität Kiel.

Thornalley, D. J., McCave, I. N., & Elderfield, H. (2010). Freshwater input and abrupt deglacial climate change in the North Atlantic. *Paleoceanography*, *25*, PA1201. https://doi.org/10.1029/2009PA001772

van Raden, U. J., Groeneveld, J., Raitzsch, M., & Kucera, M. (2011). Mg/Ca in the planktonic foraminifera *Globorotalia inflata* and *Globigerinoides bulloides* from Western Mediterranean plankton tow and core top samples. *Marine Micropaleontology*, *78*(3), 101–112.

von Langen, P. (2001). *Non spinose planktonic foraminifera (Neogloboquadrina pachyderma) cultured for geochemical and paleoceanographic applications*. Santa Barbara: University of California, Santa Barbara.

von Langen, P., Pak, D. K., Spero, H. J., & Lea, D. (2005). Effects of temperature on Mg/Ca in neogloboquadrinid shells determined by live culturing. *Geochemistry, Geophysics, Geosystems*, *6*, Q10P03. https://doi.org/10.1029/2005GC000989

Yu, J., Broecker, W. S., Elderfield, H., Jin, Z., McManus, J., & Zhang, F. (2010). Loss of carbon from the deep sea since the Last Glacial Maximum. *Science*, *330*(6007), 1084–1087.

Yu, J., & Elderfield, H. (2008). Mg/Ca in the benthic foraminifera *Cibicidoides wuellerstorfi* and *Cibicidoides mundulus*: Temperature versus carbonate ion saturation. *Earth and Planetary Science Letters*, *276*(1–2), 129–139.

Yu, J., Elderfield, H., & Hönisch, B. (2007). B/Ca in planktonic foraminifera as a proxy for surface seawater pH. *Paleoceanography*, *22*, PA2202. https://doi.org/10.1029/2006PA001347

Yu, J., Elderfield, H., Jin, Z., & Booth, L. (2008). A strong temperature effect on U/Ca in planktonic foraminiferal carbonates. *Geochimica et Cosmochimica Acta*, *72*(20), 4988–5000.

Yu, J., Thornalley, D. J., Rae, J. W., & McCave, N. I. (2013). Calibration and application of B/Ca, Cd/Ca, and δ^{11}B in *Neogloboquadrina pachyderma* (sinistral) to constrain CO_2 uptake in the subpolar North Atlantic during the last deglaciation. *Paleoceanography*, *28*, 237–252. https://doi.org/10.1002/palo.20024

Žarić, S., Donner, B., Fischer, G., Mulitza, S., & Wefer, G. (2005). Sensitivity of planktic foraminifera to sea surface temperature and export production as derived from sediment trap data. *Marine Micropaleontology*, *55*(1), 75–105.